

Centella asiatica (L.) Urban. Attenuates Cell Damage in Hydrogen Peroxide-Induced Oxidative Stress in Transgenic Murine Embryonic Stem Cell Line-Derived Neural-Like Cells: A Preliminary Study for Potential Treatment of Alzheimer's Disease

Nur Izzati Mansor^{a,b}, King-Hwa Ling^{a,c,d}, Rozita Rosli^{a,d,e}, Zurina Hassan^f,
Mohd Ilham Adenan^g and Norshariza Nordin^{a,c,d,*}

^aMedical Genetics Unit, Department of Biomedical Science, Faculty of Medicine and Health Sciences, Universiti Putra Malaysia, Serdang, Selangor, Malaysia

^bDepartment of Nursing, Faculty of Medicine, Universiti Kebangsaan Malaysia, Jalan Yaacob Latif, Cheras Kuala Lumpur, Malaysia

^cMalaysian Research Institute on Ageing (MyAgeingTM), Universiti Putra Malaysia, Serdang, Selangor, Malaysia

^dGenetics and Regenerative Medicine (ReGEN) Research Group, Faculty of Medicine and Health Sciences, Universiti Putra Malaysia, Serdang, Selangor, Malaysia

^eUPM-MAKNA Cancer Research Laboratory, Institute of Bioscience, Universiti Putra Malaysia, Serdang, Selangor, Malaysia

^fCentre for Drug Research, Universiti Sains Malaysia, Gelugor, Penang, Malaysia

^gAtta-ur-Rahman Institute for Natural Product Discovery (AuRIns), Universiti Teknologi MARA, Puncak Alam Campus, Bandar Puncak Alam, Selangor Darul Ehsan, Malaysia

Accepted 15 May 2023

Pre-press 13 June 2023

Abstract.

Background: *Centella asiatica* (L.) (*C. asiatica*) is commonly known in South East and South East Asia communities for its nutritional and medicinal benefits. Besides being traditionally used to enhance memory and accelerate wound healing, its phytochemicals have been extensively documented for their neuroprotective, neuroregenerative, and antioxidant properties.

Objective: The present study aims to investigate the effects of a standardized raw extract of *C. asiatica* (RECA) on hydrogen peroxide (H₂O₂)-induced oxidative stress and apoptotic death in neural-like cells derived from mouse embryonic stem (ES) cell line.

Methods: A transgenic mouse ES cell (46C) was differentiated into neural-like cells using 4-/4+ protocol with addition of all-trans retinoic acid. These cells were then exposed to H₂O₂ for 24 h. The effects of RECA on H₂O₂-induced neural-like cells were assessed through cell viability, apoptosis, and reactive oxygen species (ROS) assays, as well as neurite length measurement. The gene expression levels of neuronal-specific and antioxidant markers were assessed by RT-qPCR analysis.

*Correspondence to: Norshariza Nordin, PhD, Medical Genetics Unit, Department of Biomedical Science, Faculty of Medicine and Health Sciences, Universiti Putra Malaysia, 43400 Serdang,

Selangor, Malaysia. Tel.: +603 97692650, +601 92647174; E-mail: shariza@upm.edu.my.

Results: Pre-treatment with H₂O₂ for 24 hours, in a dose-dependent manner, damaged neural-like cells as marked by a decrease in cell viability, substantial increase in intracellular ROS accumulation, and increase in apoptotic rate compared to untreated cells. These cells were used to treat with RECA. Treatment with RECA for 48 h remarkably restored cell survival and promoted neurite outgrowth in the H₂O₂-damaged neurons by increasing cell viability and decreasing ROS activity. RT-qPCR analysis revealed that RECA upregulated the level of antioxidant genes such as thioredoxin-1 (*Trx-1*) and heme oxygenase-1 (*HO-1*) of treated cells, as well as the expression level of neuronal-specific markers such as *Tuj1* and *MAP2* genes, suggesting their contribution in neuritogenic effect.

Conclusion: Our findings indicate that RECA promotes neuroregenerative effects and exhibits antioxidant properties, suggesting a valuable synergistic activity of its phytochemical constituents, thus, making the extract a promising candidate in preventing or treating oxidative stress-associated Alzheimer's disease.

Keywords: Alzheimer's disease, *Centella asiatica*, mouse embryonic stem cells, oxidative stress, reactive oxygen species

INTRODUCTION

In recent years, there has been growing interest in the role of antioxidants in the prevention and treatment of neurodegenerative diseases (NDs), including Alzheimer's disease (AD). Thus, studies utilizing medicinal herbs with antioxidant and regenerative properties will be beneficial in alleviating the detrimental effects of oxidative stress. Numerous studies have shown that plant-based antioxidants serve as scavengers of free radicals and modulators of apoptosis at the cellular and molecular levels. One such plant is *Apiaceae* (previously known as *Umbelliferae*) family and the species known as *Centella asiatica* (*C. asiatica*); in Malaysia, it is also locally known as *pegaga*. *C. asiatica* is a tender creeping perennial herb of South and Southeast Asia. The whole plant (leaves, seeds, fruits, roots, stem) can be used. The plant is rich with asiaticoside (antimicrobial and neuroprotective activities), asiatic acid (neuroprotective, anticancer, and antioxidant activities), triterpenoid derivative called madecassol and triterpene (saponins and their sapogenins), flavonoids and phenolic (antioxidants activity) [1–5]. *C. asiatica* has been listed as a drug in Indian Herbal Pharmacopoeia, German Homeopathic Pharmacopoeia, European Pharmacopoeia, and Pharmacopoeia of the People's Republic of China [6]. A growing body of literature has shown that *C. asiatica* extract has been broadly tested for its pharmacological properties, such as wound healing [7–9], anxiolytic and antidepressant [10–12], neuroregenerative, neuroprotective, memory-enhancing activities [1, 13–19], as well as antioxidant and anti-inflammation [20–22]. Therefore, it has been identified as a suitable candidate that can be used as an adjunct treatment for NDs, especially AD.

In vitro model of diseases has been extensively used for the screening of pharmacological compounds or medicinal herbs. The selection of cells to be employed plays an important role in the development of the ideal model for specific diseases, including AD. Current available *in vitro* AD models, including PC12 and SH-SY5Y cell lines, lack many of the crucial features to mimic the *in vivo* condition, including neuronal morphology, functional mature neurons, signaling pathways encompassing cell division and survival, as well as apoptosis pathway. Several studies have shown the capability of stem cells to differentiate into various types of cells and their ability to secrete a wide range of trophic factors, making them the best treatment for degenerative diseases [23]. Furthermore, stem cells have become valuable tools in the establishment of *in vitro* models of AD and to study therapeutic strategies, owing to their capability to differentiate into any type of cells.

To expand the choice of stem cells used as the prospect cells for establishing AD *in vitro* models, we are exploring and manipulating the properties of mouse embryonic stem cell line, 46C. 46C is a transgenic mouse embryonic stem cell line carrying a green fluorescent protein (*GFP*) gene knocked-in in the open reading frame of a marker for neural precursor cells (NPCs), *Sox1* [24]. 46C-derived neural-like cells were obtained by 4-/4+ protocol through the formation of multicellular aggregates, embryoid bodies (EBs), with the addition of *all-trans* retinoic acid as the neural inducer [25].

In our study, H₂O₂ was used to induce neurotoxicity in neural-like cells derived from 46C to elevate the intracellular reactive oxygen species (ROS) activity, leading to oxidative stress. The correlation between H₂O₂ and oxidative stress model is well documented

in previous works. In biological systems, H_2O_2 is well recognized as the inducer of ROS and apoptosis, and in fact, H_2O_2 itself is also ROS. H_2O_2 is also produced as a by-product of dismutation superoxide anions (O_2^-) during cellular metabolism by superoxide dismutase [26]. In AD, H_2O_2 is produced by amyloid- β peptide, which is responsible for senile plaque formation [27, 28] and tau protein, which is the major component of neurofibrillary tangles [29]. Several factors influence H_2O_2 -induced apoptotic cell death by causing nuclear condensation and DNA fragmentation, as well as mitochondrial dysfunction [30] and activation of caspase 3 [31], and regulation of pro-apoptotic Bcl2 family [32]. Therefore, exogenous H_2O_2 was frequently used in the *in vitro* study for the fact that it induces oxidative stress conditions comparable to *in vivo* models particularly related to AD.

The novelty of the project relies on the aim to evaluate the neuroregenerative effect of the raw extract of *C. asiatica* (RECA) on oxidative stress-induced neural-like cells differentiated from murine embryonic stem cells as opposed to commonly used cancer cell lines, such as human neuroblastoma cell line (SH-SY5Y) and rat pheochromocytoma (PC12) cells. The neuroregenerative effect of RECA was evaluated based on the regeneration of neurite outgrowth, cell viability, intracellular ROS, number of apoptotic cells, and antioxidant gene expression of H_2O_2 -induced oxidative stressed 46C-derived neural-like cells. Our work also demonstrates the importance of the synergistic effect of compounds of natural plant extract over pure pharmacological compounds as an alternative adjunct that could be safely consumed as medicines.

MATERIALS AND METHODS

Study design

The establishment of *in vitro* neurodegenerative models using neural-like cells derived from a transgenic mouse embryonic stem cell line (46C) was carried out. Routine cell culture and neural differentiation assay protocols were carried out as described in the following sections. Cell characterization and neurogenic potential of 46C were conducted by immunocytochemistry and flow cytometry analyses were performed in accordance with the manufacturer's instructions. Next, the 46C-derived neural-like cells (DIV 12 upon neural induction) were exposed to H_2O_2 for 24 h in a concentration-dependent manner.

The doses of H_2O_2 were selected based on previous work [25]. After 24 h treatment with H_2O_2 , the 46C-derived neural-like cells were rested for 24 h before being treated with RECA for another 48 h (DIV 14 upon neural induction); dbcAMP was used as positive controls. After 48 h treatment with RECA, the 46C-derived neural-like cells were left rested for 24 h before being evaluated for cell morphology and viability (MTT assay), intracellular ROS production (H_2DCF -DA assay), number of apoptotic cells, antioxidant gene expression, and neurite outgrowth (DIV 17 upon neural induction).

Cell culture

The 46C mES cells were a gift from Professor Dr. John Mason (University of Edinburgh, United Kingdom). The cell line was maintained in GMEM (BHK-21; GibcoTM; ThermoFisher Scientific, USA) supplemented with 15% (v/v) fetal bovine serum (FBS; GibcoTM; ThermoFisher Scientific, USA), 1% MEM non-essential amino acids (GibcoTM; ThermoFisher Scientific, USA), 1 mM sodium pyruvate (GibcoTM; ThermoFisher Scientific, USA), 0.1 mM 2-mercaptoethanol (GibcoTM; ThermoFisher Scientific, USA), 2 mM L-glutamine (Gibco) and 10 ng/mL human recombinant leukemia inhibitory factor (LIF 1010; Merck Millipore, USA). The cells were seeded at a cell density of 4.0×10^4 cells/cm² into 25 cm² cell culture flasks (TPP) coated with 0.1% (w/v) gelatin (Sigma-Aldrich, USA). The gelatin-coated flasks or plates were prepared by pre-coating with gelatin for at least 5 min before cell seeding. The cells were incubated at 37°C, 5% CO₂, and 90% humidity (AutoFlow IR Water-jacketed CO₂ Incubator, US). The cells were sub-cultured every other day when the cells were 70–80% confluent.

Neural differentiation assay through EB formation (–4/+4 protocol)

Neural differentiation assay was carried out through the spontaneous formation of multicellular aggregates, known as EBs, using 4–/4+ protocols adapted from Mansor et al. [25] with the addition of all-trans retinoic acid as the neural inducer. Figure 1 illustrates steps in 4–/4+ protocol.

Briefly, 5.0×10^6 undifferentiated stem cells were seeded in 100 mm Petri dishes for 4 days without LIF, followed by another 4 days in the presence of all-trans retinoic acid (Sigma) (4–/4+ induction). The medium was changed every two days. At the end of the

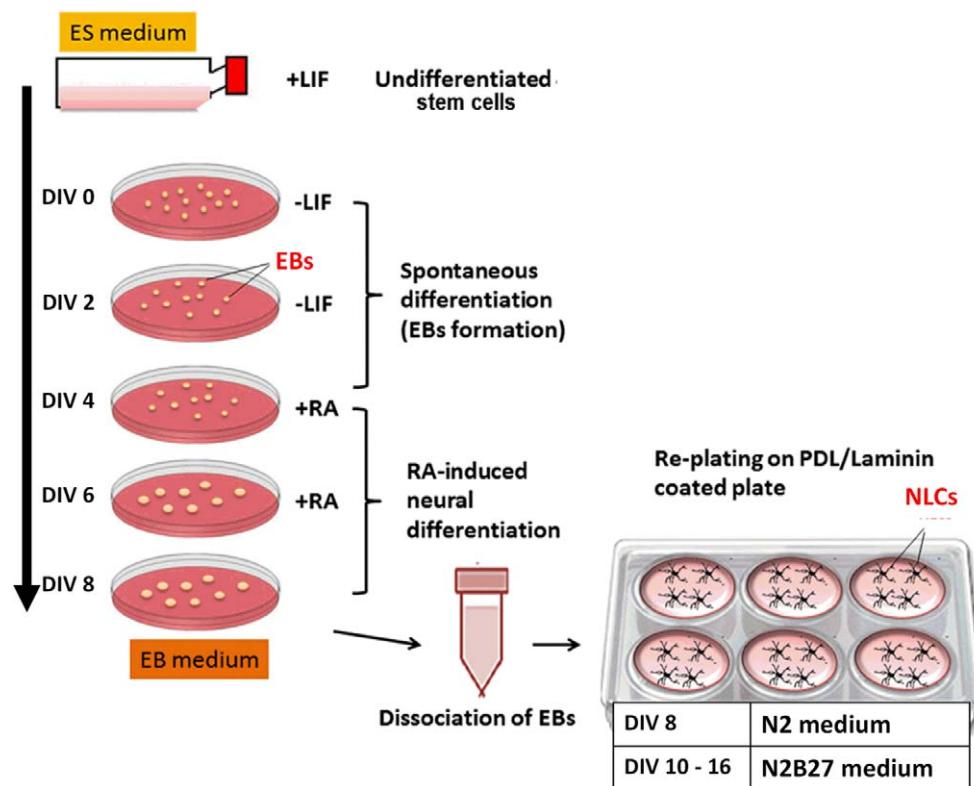


Fig. 1. Neural induction methods, 4-/4+ protocol. ES medium, embryonic medium; EBs, embryoid bodies; DIV, day *in vitro* (in culture); RA, retinoic acid; PDL, Poly-D-lysine; NLCs, neural-like cells.

induction period (DIV 8), the EBs were dissociated into single cells with $4\times$ trypsin-EDTA and plated on Poly-D-Lysine (PDL)/laminin (Sigma-Aldrich, USA) coated plates at the density of $2.0\text{--}3.0 \times 10^4$ cells/cm². The neural differentiation assay was carried out over 14–16 post-plating (DIV 14–16).

Immunocytochemistry

Immunocytochemistry (ICC) was prepared in 24-well plates. The attached cells were fixed in 4% w/v paraformaldehyde (PFA), 50 mM NaOH, 1 \times PBS) for 30 min, followed by permeabilization in 1% Triton-X100 for 15 min at room temperature (RT). Cells were then incubated in blocking solution (1% bovine serum albumin, 1% goat serum, 0.1% Tween-20 in 1 \times PBS) for 30 min before incubation with primary antibody at 4°C overnight. After washing with 1 \times PBS, the cells were then incubated with fluorochrome-conjugated secondary antibody for 2 h at RT in the dark. After washing, the cells were counterstained with DAPI (Sigma-Aldrich, USA) for 10 min at RT. The cells were then left in 1 \times PBS in the

dark until visualization with an inverted fluorescent microscope (Olympus IX51, Japan). The antibodies used in this study are listed in Table 1.

Flow cytometry

Pluripotency protein markers: Expression of Oct4, Nanog, and Sox-2 were characterized using flow cytometry to detect pluripotency properties and the stemness of undifferentiated stem cells. The antibodies used in this study are listed in Table 1.

Neuronal protein markers: Flow cytometry was performed to characterize neuronal and glial cell expression in neural-like cells derived from 46C cells. The neural markers used were: class III β -tubulin for the detection of post-mitotic neurons; microtubule-associated protein 2, MAP2, for the detection of mature neurons; and glial fibrillary acidic protein, GFAP, for the detection of glial cells, mainly astrocytes in 46C-derived neural-like cells. The antibodies used in this study are listed in Table 1.

Briefly, the undifferentiated stem cells were grown to 80% confluence. Meanwhile, the 46C-

Table 1
Primary and secondary antibodies and the dilution factors used

Primary Antibody		Secondary Antibody	
Antibody and catalogue No.	Dilution	Antibody and catalogue No.	Dilution
Rabbit Anti-Oct4 (ab18976; Abcam, UK)	1:300 (Flow cytometry) 1:200 (ICC)	Alexa Fluor 594 Goat Anti-Rabbit IgG (A11037; Thermo Fisher, USA)	1:300 (Flow cytometry) 1:200 (ICC)
Rabbit Anti-Nanog (SC-33760; Santa Cruz Biotechnology, USA)	1:200 (Flow cytometry) 1:200 (ICC)		
Rabbit Anti-GFAP (ab7260; Abcam, UK)	1:300 (Flow cytometry) 1:200 (ICC)		
Rabbit Anti-Class III β -Tubulin (ab18207; Abcam, UK)	1:300 (Flow cytometry) 1:200 (ICC)	Alexa Fluor 488 Goat Anti-Rabbit IgG (A11034, Thermo Fisher, USA)	1:300 (Flow cytometry) 1:200 (ICC)
Rabbit Anti-CHAT (ab68779; Abcam, UK)	1:300 (Flow cytometry) 1:200 (ICC)		
Mouse Anti-Sox2 (ab79351; Abcam, UK)	1:300 (Flow cytometry) 1:200 (ICC)	Alexa Fluor 488 Goat Anti-Mouse IgG1, kappa (A21121, Thermo Fisher, USA)	1:300 (Flow cytometry) 1:200 (ICC)
Mouse Anti-Map2 (ab11267; Abcam, UK)	1:200 (Flow cytometry)		
Mouse Anti-Map2 (13–1500; Invitrogen, USA)	1:250 (ICC)		

derived neural-like cells were harvested on the day they reached maturation (DIV 14). The cells were trypsinized from the tissue flasks by mild trypsinization prior to fixation and permeabilization with ice-cold methanol for 40 min at 4°C. The cells were centrifuged at 1000 rpm, washed with 1 × PBS twice, and then incubated with primary antibodies in a blocking solution for 1 h at RT. The cells were then washed with 1 × PBS twice and incubated with secondary antibody (1:300; Alexa Fluor 488 Goat Molecular probes® anti-rabbit or anti-mouse IgG H+L; Invitrogen, USA) for 30 min at RT, in the dark. The cells were resuspended in 500 μ L of 1 × PBS before analysis using a flow cytometer (LSR Fortessa; BD Biosciences, USA). Fluorescence intensities of 10^4 cells were acquired and analyzed using FACs Diva Software.

Source of plant material

Sample preparation: Standardized RECA was obtained from Professor Dr. Mohd Ilham Adenan, from Atta-ur-Rahman Institute for Natural Product Discovery (AuRIns), Universiti Teknologi Malaysia (UiTM), Selangor, Malaysia. A voucher specimen (CA-K017) was given by the curator of AuRIns, UiTM. The extraction process to yield standardized

RECA was mentioned previously [21, 33]. RECA has been shown to consist of all four bioactive components of *C. asiatica* (L), which are madecassoside (0.0060%), asiaticoside (0.0035%), madecassic acid (0.0020%), and asiatic acid (0.017%). Additionally, RECA also contains 206.73 ± 5.53 mg/100 g gallic acid equivalent (GAE) of total phenolic content and is found to have $57.70 \pm 0.78\%$ antioxidant activity through DPPH (2,2-diphenyl-1-picrylhydrazyl) [33]. 10 mg of lyophilized RECA was weighed (Mettler Toledo, USA) and dissolved in 1 mL of water. After that, the extract was filtered by using a 0.22 μ m syringe filter (Millipore, USA) for sterilization and elimination of insoluble residues. Eight (8) different concentrations of RECA (0.1, 1.0, 10.0, 100, 250, 500, 750, and 1000 μ g/ml) were then prepared.

Effect of RECA on cell viability of neural-like cells derived from 46C

Treatment with RECA was conducted on day 14 post-plating 46C-derived neural-like cells (4-/4+ protocol). 46C cells were seeded in 24-well plates at a cell density of $2.0\text{--}3.0 \times 10^4$ cells/cm² in DMEM/F12 supplemented with N2 and Neurobasal supplemented with B27 medium (ratio 1:1). When the cells reached their maturation (day 14 upon

neural induction using 4–/4+ protocol), the cells were exposed to RECA for 48 h. Cell morphology was observed after 48 h of treatment via IX51 Fluorescence Inverted Microscope (Olympus, USA). Cell viability was evaluated by using 3-(4,5-dimethylthiazol-2-yl)-2,5-diphenyl tetrazolium bromide (MTT) colorimetric assay. In post-treatment with H₂O₂, MTT solution was added into all wells and incubated for 4 h. Following incubation, the mixture of MTT solution and medium in the wells was discarded and substituted with 100 µL of DMSO to solubilize the purple formazan crystal. The cell was then subjected to an ELISA microtiter plate reader (AsysHighTech UVM340, Biochrom, UK) at 570 nm wavelength with a reference of 630 nm wavelength to measure the cell absorbance. Statistical analysis was done using a one-way ANOVA. All statistical analyses were conducted by GraphPad Prism version 6.

Post-treatment with RECA on H₂O₂-induced oxidative stress in neural-like cells derived from 46C cells

To determine the neuroregenerative effect of RECA on H₂O₂-induced oxidative stress in neural-like cells derived from 46C cells, cell toxicity was induced with 1500 µM H₂O₂ for 24 h. The cells were then left to rest in an H₂O₂-free medium (N2B27 medium without H₂O₂) for another 24 h. The doses of H₂O₂ were selected based on previous work [25]. The H₂O₂-damaged neural-like cells were then exposed to RECA at concentrations of 1 and 10 µg/mL for 48 h, followed by being cultured in a normal medium without RECA for another 24 h. dbcAMP was used to serve as a control.

Assessment of cell apoptosis

Cellular apoptosis was determined using Annexin V-FITC/Propidium Iodide (PI) apoptosis detection kit (Sigma Aldrich, USA), according to the manufacturer's instructions, and was analyzed using flow cytometry, to determine the the percentage of apoptotic cells after treatments with H₂O₂ and RECA. Cells were treated as stated above. Then, the cells were harvested, incubated with Annexin V-FITC and Propidium Iodide (PI), and analyzed at 525 nm for FITC and 630 for PI with a flow cytometer (LSR Fortessa; BD Biosciences, USA). Early apoptotic cells were defined as those cells that expressed only Annexin V/FITC. Meanwhile, late apoptotic cells

expressed both Annexin V/FITC and PI. Dead cells expressed only PI. Apoptosis assay was run at least twice, with technical triplicates. The fluorescence intensity of 10⁴ cells was acquired and analyzed using FACs Diva Software. For statistical analysis, one-way ANOVA was used (GraphPad Prism version 6).

Measurement of intracellular reactive oxygen species

Intracellular ROS was measured using H₂DCF-DA (Thermo Fisher Scientific, USA, cat no#D399). The cell-permeable 2',7'-dichlorodihydrofluorescein diacetate (H₂DCF-DA) diffuses and is deacetylated by cellular esterases to non-fluorescent 2',7'-dichlorodihydrofluorescein (DCFH) which reacts with ROS (which includes hydroxyl, peroxy and other ROS activities within a cell) to form a highly fluorescent 2',7'-dichlorodihydrofluorescein (DCF).

Briefly, the cells were washed twice with 1× PBS followed by pre-incubation with the oxidant (H₂O₂) and incubated for 24 h. The cells were then left to rest in the normal medium for another 24 h. The H₂O₂-treated neural-like cells were then exposed to RECA (1 and 10 µg/mL), or dbcAMP (50 µM) for 48 h. After 48 h treatment with RECA, the medium was replaced with the normal medium (without RECA) for another 24 h. Then, the cells were pre-incubated with 10 µM DCFH-DA (final concentration) in 500 µL of N2B27 medium for 30–45 min at 37°C. The supernatant was removed, and the cells were washed twice with 1× PBS. For flow cytometry analysis, the DCFH-DA-treated cells were trypsinized and then resuspended in 500 µL of 1× PBS, before DCF analysis using a flow cytometer (LSR Fortessa; BD Biosciences, USA). H₂DCF-DA fluorescence intensity of 10⁴ cells was acquired and analyzed using FACs Diva Software.

Gene expression analysis

To determine the effect of RECA as an antioxidant, total RNA from treated cells was isolated using RNeasy mini plus kit (Qiagen, Germany), according to the manufacturer's protocol under RNase-free conditions and quantitated using Nanodrop (Nnovue). Reverse transcription of genes was performed on 0.5–1.0 µg of total RNA using a Reverse Transcription System kit (Nanohelix, Korea), according to manufacturer's protocols and RT-qPCR was performed using RotorGene Sybr Green PCR kit (Qiagen). The primer sequences are listed in Table 2.

Table 2
List of primers and their properties

Gene		Primers (5' → 3')	GC (%)	Tm (°C)	Amplicon size (nt)
<i>Tuj1</i>	Forward	ATGGACAGTGTTCGGTCTGG	55	60	147
	Reverse	CCGCACGACATCTAGGACTG	60	60	
<i>MAP2</i>	Forward	TCCTCTCTACCTCCGCTTCC	60	60	126
	Reverse	TCACAGCTTACTCGCAGAGC	55	60	
<i>Trx-1</i>	Forward	CTGCTTTTCAGGAAGCCTTG	50	57	203
	Reverse	TGTTGGCATGCATTTGACTT	40	57	
<i>HO-1</i>	Forward	CACGCCTACACCCGCTACCT	65	60	209
	Reverse	TCTGTCACCCTGTGCTTGAC	55	64	
β -actin	Forward	CCTGTCAGCAATGCCTGGGT	60	63	151
	Reverse	CCAGCCTTCCTTCTGGGTA	55	59	

The primer pairs of genes of interest were synthesized by First Base (Malaysia) and designed using Roche Universal Probe Library from the following website: https://lifescience.roche.com/en_my/brands/universal-probe-library.html. The sequence was blasted using NCBI primer Blast tool software from the following website: <https://www.ncbi.nlm.nih.gov/tools/primer-blast/>.

RT-qPCR reactions were performed in LightCycler[®]480 Instrument II (Roche). RT-qPCR was carried out by amplifying the cDNA at initial denaturation at 95°C for 5 min, followed by amplification at 35–40 cycles at 95°C for 15 s (denaturation), 58–60°C for 15 s (annealing) and at 72°C for 15 s (elongation). Data were normalized to the β -actin values. All data are reported as the mean \pm SEM, $n = 3$. For statistical analysis, one-way ANOVA and *post-hoc* Bonferroni test were used (GraphPad Prism version 6).

Measurement of neurite length

The neurite length was measured as the distance between the cell soma and the tip of its longest neurite [34]. The neurites of 15 cells in 4-5 random fields were averaged to evaluate the neurite outgrowth for each treatment. The cells with neurites were manually counted, and measurements of the neurite length were then analyzed using Neuron J (Maryland, USA).

RESULTS

Propagation and characterization of 46C

In this study, a transgenic mouse embryonic stem cell line (46C) was propagated in cultures. The quality of 46C cells was assessed to determine the efficiency of the neural differentiation of the cells. With the proper culturing technique, high-quality stem cells

were achieved, as characterized by the increased nucleus-to-cytoplasm ratio and large nucleus with multiple nucleoli (Fig. 2a). Population doubling time (PDT), which is the time taken for the cell to double in culture, for 46C cells was 20.5 ± 0.5 h ($n = 12$) from randomly chosen passages within P25 – 40 (data not shown).

The 46C cells were qualitatively analyzed by ICC for the expression of three fundamental pluripotency-associated markers; Octamer-binding protein, Oct4, homeobox protein, Nanog and SRY-box 2, Sox2. High expressions of these transcription factor proteins were observed in undifferentiated 46C cells, localized in the nucleus as shown in Fig. 2b, signifying the biological activity of the cells. DAPI was used to counterstain the nuclei. The expression of pluripotency markers was then quantified by flow cytometry. 46C cells were evaluated and presented in a dot-plot, as illustrated in Fig. 2c. Interestingly, the expression of these pluripotency markers was distinctly high in undifferentiated 46C cells. 46C cells were observed to express high Oct4 ($99.9 \pm 0.03\%$), Nanog ($83.3 \pm 0.4\%$), and Sox2 ($81.2 \pm 0.3\%$), indicating high the pluripotency status of the cells. Another important characteristic of pluripotency potential of cells is the ability of the cells to spontaneously form multicellular aggregates, called EBs, in the absence of LIF. As demonstrated in Fig. 2d, 46C cells started to form cell aggregates on day 2 upon the removal of LIF. These multicellular aggregates matured on days 4 and 6, as revealed by smooth-edged spherical morphology and cavitation (dark area in the middle of the EBs, indicating the population of dead cells). These results indicated good-quality pluripotent stem cells.

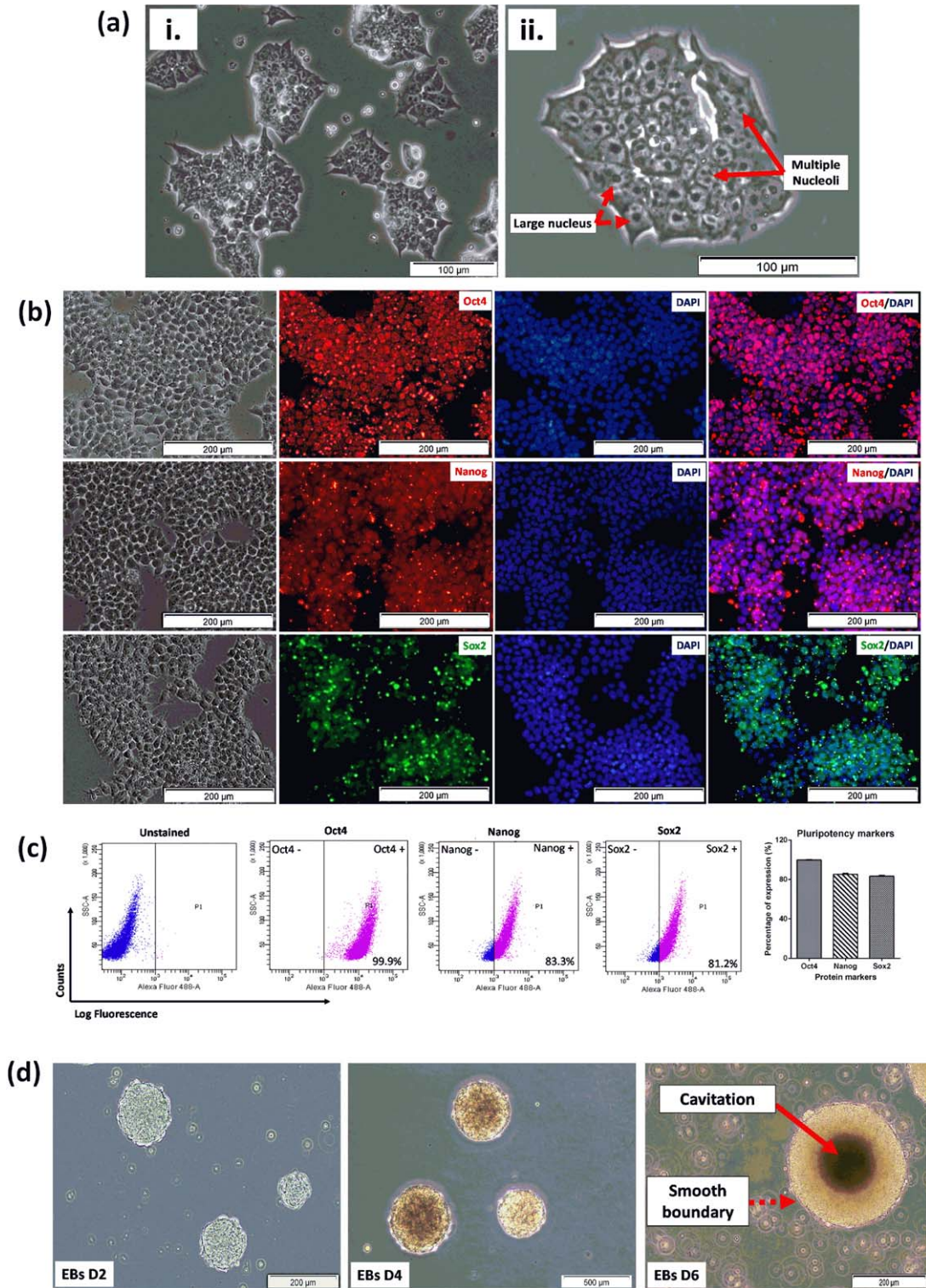


Fig. 2. (Continued)

Fig. 2. (a) Morphological characteristics of undifferentiated 46C cells. (i-ii) Good quality 46C cells exhibit a high nucleus-cytoplasm ratio (indicated with a dashed arrow) with multiple nucleoli (indicated with solid arrows) in culture. (b) Immunostaining of pluripotency-associated protein markers. The fundamental pluripotency markers such as Oct4, Nanog, and Sox2 were expressed in undifferentiated 46C cells. High expressions of Oct4, Nanog, and Sox2 were observed in undifferentiated 46C cells, localized in the nuclei, indicating the pluripotency of the cells was still maintained in the culture. DAPI was used to counterstain the nuclei. The scale bars represent 100 μm for micrographs. (c) Representative flow cytometric analysis of pluripotent transcription markers (Oct4, Nanog, and Sox2), for detecting pluripotency state of 46C cells. All data are presented as mean \pm SEM ($n = 3$). The gating for 46C-derived neural-like cells was based on its respective unstained control. (d) Spontaneous formation of good quality embryoid bodies (EBs) that were presented with cavitation process, smoothness of the boundary, and acceptable diameter (100 to 300 μm , as indicated by the scale bars 200 μm and 500 μm), indicated the presence of pluripotent stem cells. Random micrographs were taken from EBs culture on days 2, 4, and 6; chosen passages within P25 – 40.

The neurogenic potential of 46C cells

The neurogenic potential of 46C cells was investigated by screening their ability to spontaneously differentiate into a neural lineage. 46C cells were differentiated into neural-like cells using neural induction protocol, namely the cell suspension method through the formation of EBs (4-/4+; non-adherent culture) protocol. All results shown in this study were obtained up to fourteen days in a culture which is often called day *in vitro* (DIV). The morphology of neural-like cells was monitored on DIV 2, DIV 6, and DIV 14. Figure 3 illustrates the morphology of 46C cells undergoing directed differentiation up to the mature neurons stage. Morphologically, in our hands, both methods were able to generate cells with neural-like morphology for 46C cells.

The quality of EBs is an important benchmark to indicate success in generating good neurons, as previously depicted in Fig. 2d. Neural induction was carried out by treating DIV 4 EBs with all-trans retinoic acid on DIV 4 to DIV 8 EBs. Qualitative analysis by visualization of *Sox1*^{eGFP} expression under fluorescence inverted microscope showed the highest intensity of GFP on day 6 EBs (Fig. 3a). *Sox1* is a marker for NPCs. Expression of GFP marks the presence of NPCs. NPCs in EBs were isolated using chemical dissociation (4 \times trypsin-EDTA) and then plated onto PDL/Laminin-coated dish. Cells with obvious neural-like morphology appeared after day 2 post-plating onto PDL/Laminin-coated dish (DIV 10). We observed the appearance of a heterogeneous population of cells with neuronal morphologies, including single-cell soma or a clump of cells, bearing multiple neurites, characterized by short and thin claw-like projections. The cells were then expanded until day 6 post-plating poly-D-lysine (PDL)/Laminin-coated dish (DIV 14), and we observed the appearance of the highly dense network of claw-like projections and multiple recurrent branching of neurite projections. Various degrees of neurite complexity were observed,

suggesting various types of neural-like cells at different stages of maturation.

To detect specific neuronal and glial protein markers, 46C-derived neural-like cells differentiated from the 4-/4+ protocol were selected. 46C cells were capable of differentiating into highly pure neural-like cells using the 4-/4+ protocol. We confirmed this by immunostaining (Fig. 3b) and flow cytometry (Fig. 3c) analyses of the expression of neural-specific protein markers such as post-mitotic neuron (class III beta (β)-tubulin, Tuj1), mature neuron (microtubule-associated protein 2, Map2), cholinergic neuron (choline acetyltransferase, CHAT) and glial cell, mainly astrocytes (glial fibrillary acidic protein, GFAP). Immunostaining showed that 46C-derived neural-like cells differentiated from 4-/4+ protocol were positive to Tuj1, MAP2, and CHAT, as well as GFAP staining, marking the presence of the heterogeneous population of cells in culture. Data from flow cytometry analysis showed that the percentage of Tuj1-positive cells in the differentiated 46C cells was as high as $97.1 \pm 0.9\%$. While the percentage of Map2-, CHAT-, and GFAP-positive cells in the differentiated 46C cells after day 14 of neural induction was $70.0 \pm 1.4\%$, $33.5 \pm 1.0\%$, and $55.5 \pm 1.9\%$, respectively.

Effect of H₂O₂ on cell morphology and viability of neural-like cells derived from 46C cells

An initial experiment was conducted to determine the tolerance concentration of 46-derived neural-like cells against H₂O₂ insults for 24 h treatment. In this study, the 4+/4- protocol was used to differentiate the 46C into neural-like cells. A significant decrease in cell viability with an increase in H₂O₂ concentrations. Moreover, the treatment concentrations that are capable of killing 50%, of neural-like cells (IC₅₀) were inferred from the plotted graph. As shown in Fig. 4a, approximately $53.3 \pm 2.4\%$ ($p < 0.0001$) of 46C-derived neural-like cells remained viable when

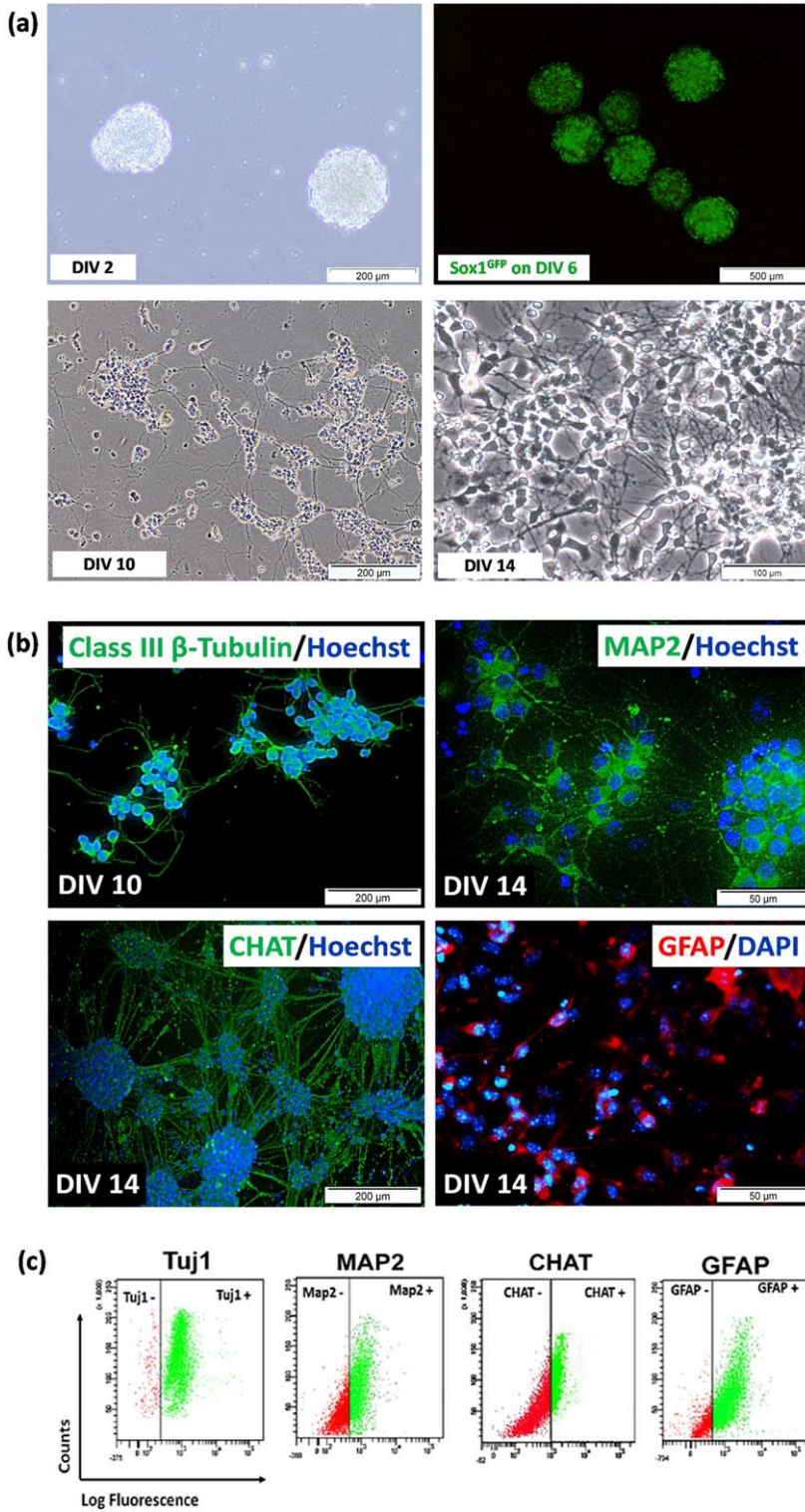


Fig. 3. (Continued)

Fig. 3. (a) Differentiation of 46C cells after neural induction using 4-/4+ protocol from DIV 2 to DIV 14. The cells underwent progressive loss of pluripotency and eventually developed into neural-like cells with the formation of projections and making connections with adjacent cells. A few of 46C cells loss (i.e., died, detached, etc.) during the neural differentiation process, and the remaining survived to the late neural differentiation stage (DIV 14). (b) Immunostaining and (c) representative of flow cytometric analysis of neural-specific markers after neural differentiation of 46C cells from 4-/4+ protocols. Immunostaining of class III β -tubulin (Tuj1) was from day 2 neural-like cells post-plated onto PDL/Laminin-coated plates (DIV 10); meanwhile, immunostaining of MAP2, CHAT, and GFAP was from day 6 neural-like cells post-plated onto PDL/Laminin-coated plates (DIV 14). Nuclei were counterstained with DAPI or Hoechst 33342 (blue). The scale bars represent 50 (magnification: 40 \times) and 200 μ m (magnification: 20 \times) for micrographs. The gating for 46C-derived neural-like cells was based on the respective unstained controls.

treated with 1500 μ M of H_2O_2 for 24 h. Therefore, pre-treatment with 1500 μ M of H_2O_2 was selected for 46C-derived neural-like cells for the subsequent neuroregenerative experiments, as this concentration induced 50% injury in neural-like cells; thus, therapeutic effects of the natural product can be established. Morphology of untreated 46C-derived neural-like cells appeared to have complete intact membranes, with small cell bodies and elongated neurite projections. In contrast, incomplete cellular membranes, some cells were shrunken with abnormal morphology and damaged neurite projection were observed in the H_2O_2 -treated 46C-derived neural-like cells. The degree of cell damage was exacerbated by the increasing level of H_2O_2 , as previously reported in Fig. 4b.

In addition to the cell viability and morphological assessments, the apoptotic rate was further determined by Annexin V/FITC assay to determine the degree of H_2O_2 -induced apoptosis. Neural-like cells derived from 46C cells were pre-incubated with H_2O_2 for 24 h prior to flow cytometric analysis. As shown in Fig. 4c, the percentage of apoptotic cells increased when treated with H_2O_2 . The apoptotic percentage was $4.8 \pm 0.7\%$ in the untreated neural-like cells derived from 46C cells. As shown in Fig. 4d, H_2O_2 -treated 46C neural-like cells significantly exhibited 20% increment in apoptotic rates, which was $24.1 \pm 4.7\%$ ($p < 0.001$), compared to untreated 46C-derived neural-like cells. These findings suggest that 1500 μ M of H_2O_2 can cause cell toxicity and apoptosis. Although the H_2O_2 concentration used in this *in vitro* oxidative stress model is high when compared to previous works using different cell lines, this concentration of H_2O_2 is optimal for the operation of this study due to the numerous response and resistance to H_2O_2 within the heterogeneous cell population in the culture.

Effect of RECA on the cell viability of 46C-derived neural-like cells

Next, we evaluated the cytotoxic effect of RECA on the 46C-derived neural-like cells at the concentration range from 0.1 to 1000 μ g/mL for 48 h. As depicted in Fig. 5a, the effect of RECA against cell viability was dose-dependent. The increase in cell viability was observed after supplementation with RECA at the concentration of 1 μ g/mL, and 10 μ g/mL ($p < 0.05$) for 48 h, as compared to untreated cells (0 μ g/mL). However, more cytotoxicity effects on cell growth were observed when the concentration of RECA was increased. The viability of 46C-derived neural-like cells was reduced at the concentration between 100 to 500 μ g/mL, resulting in minimal toxicity to 46C-derived neural-like cells with approximately 70–80% survival. RECA at the higher concentration (750 and 1000 μ g/mL) significantly inhibited the growth of 46C-derived neural-like cells. Furthermore, the IC_{50} was approximately 600 μ g/mL. The results showed that the inhibitory effect of RECA on the cell viability of 46C-derived neural-like cells was associated with concentration dose. It was found that the increase in the doses of RECA up to 500 μ g/mL had minimal cytotoxic effects against 46C-derived neural-like cells. Microscopic analysis was carried out to assess the morphological changes of 46C-derived neural-like cells upon treatment with RECA for 48 h. The concentration of 1 and 10 μ g/mL of RECA exhibited an increase in neurite number and branches in 46C-derived neural-like cells. More neurites extending from cell soma were observed, suggesting neurite outgrowth activity (Fig. 5b).

Effect of RECA on the cell viability and apoptosis in H_2O_2 -induced oxidative stressed neural-like cells differentiated from 46C

Neurites of 46C-derived neural-like cells treated with 1500 μ M H_2O_2 were severely damaged, and

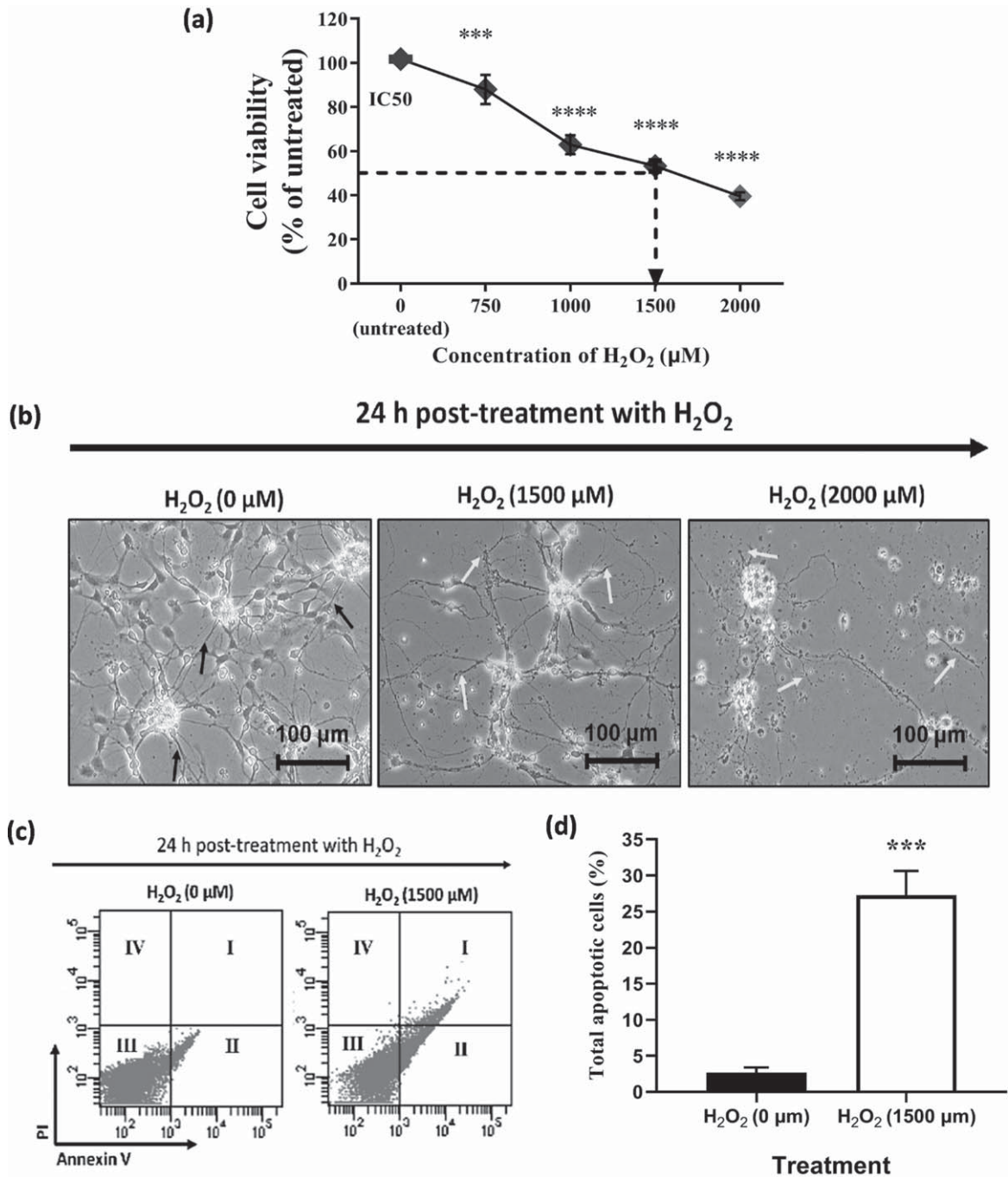


Fig. 4. The effect of H₂O₂ on the (a) cell viability and (b) morphology of neural-like cells derived from 46C cells. The effect of H₂O₂ on 46C-derived neurons is expressed as the percentage of cell viability by MTT assay. The morphology of untreated neural-like cells (0 µM H₂O₂) with neurite projections (indicated by black arrows) and 1500 µM H₂O₂-treated neural-like cells, after 24 h treatment. Neurite projections were damaged in neuronal culture treated with H₂O₂ (indicated by yellow arrows). The scale bars represent 100 µm for micrographs (magnification:20×). The effect of H₂O₂ on the apoptotic rates in 46C-derived neural-like cells is shown in (c), and in (d) the values are represented in the percentage of apoptotic cells. Data are presented as mean ± SEM (*n* = 3), where *** indicates *p* < 0.001 (significantly different from untreated cells) (Student's *t*-test). I, late apoptotic cells, which expressed Annexin V/FITC and PI; II, early apoptotic cells, which expressed only Annexin V/FITC; III, live cells, which did not express any stains; and IV, dead cells, which expressed only PI.

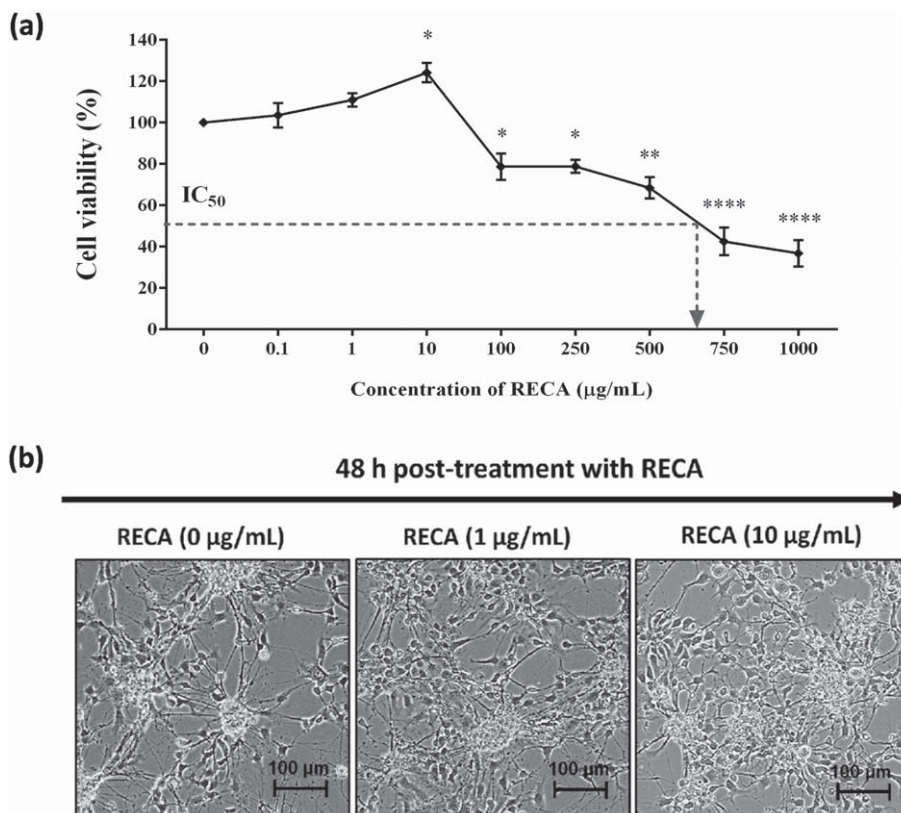


Fig. 5. (a) Cell viability of RECA on neural-like cells derived from 46C cells by MTT assay. Mature neural-like cells were exposed to different concentrations of RECA for 48 h. Data are expressed as the percentage of mean \pm SEM ($n=3$), where **** indicates $p<0.001$, ** indicates $p<0.01$, and * indicates $p<0.05$ (One way ANOVA: Tukey's test multiple comparisons) compared to untreated neural-like cells (0 $\mu\text{g/mL}$ of RECA). (b) Representative microscopy images of 46C-derived neural-like cells treated with 0, 1, 10 $\mu\text{g/mL}$ of RECA. Note the increase in neurite length and the number of branches in cells treated with RECA. The scale bars represent 100 μm for micrographs (magnification 20 \times).

the number of viable cells decreased to approximately 50% compared to untreated neural-like cells. To investigate whether RECA confers regeneration against H_2O_2 -induced 46C-derived neural cell damage, first, we detected the cell viability of neural-like cells after incubation with RECA for 48 h at concentrations of 1 and 10 $\mu\text{g/mL}$. We found that 1 $\mu\text{g/mL}$ ($p<0.05$) and 10 $\mu\text{g/mL}$ ($p<0.001$) of RECA significantly restored the cell viability of damaged neurons and increased survival rates of H_2O_2 -treated neural-like cells (Fig. 6b). Upon treatment with 1 and 10 $\mu\text{g/mL}$ of RECA for 48 h, the neurites of damaged neural-like cells started regenerating, as noted in the neurite extension when compared to H_2O_2 -treated neural-like cells alone (Fig. 6c). Normal morphologic features were observed in the untreated group. Cell morphology changed after treatment with H_2O_2 alone. The characteristic features of H_2O_2 -induced cytotoxicity include a decrease in cell number and

the presence of neurites degeneration. Co-treatment with RECA ameliorated the H_2O_2 -induced cell damage. RECA could have the ability to restore cell survival by increasing cell viability in the damaged neurons (Fig. 6c). Microscopic analysis was carried out, as shown in Fig. 6d, to assess the morphological changes of 46C-derived neural cells upon treatment with RECA for 48 h. At 48 h post-treatment with RECA at both concentrations (1 and 10 $\mu\text{g/mL}$) resulted in cells with obvious neuronal morphology with long, extensively branched neurites. Meanwhile, slower morphological changes were observed in those treated with H_2O_2 alone.

Following 48 h treatment with RECA or dbcAMP, the cell apoptosis rate in damaged neural-like cells was then analyzed by Annexin V FITC/PI assay. As illustrated in Fig. 6c, RECA treatment caused remarkable changes in the apoptosis and viability of H_2O_2 -treated cells, which con-

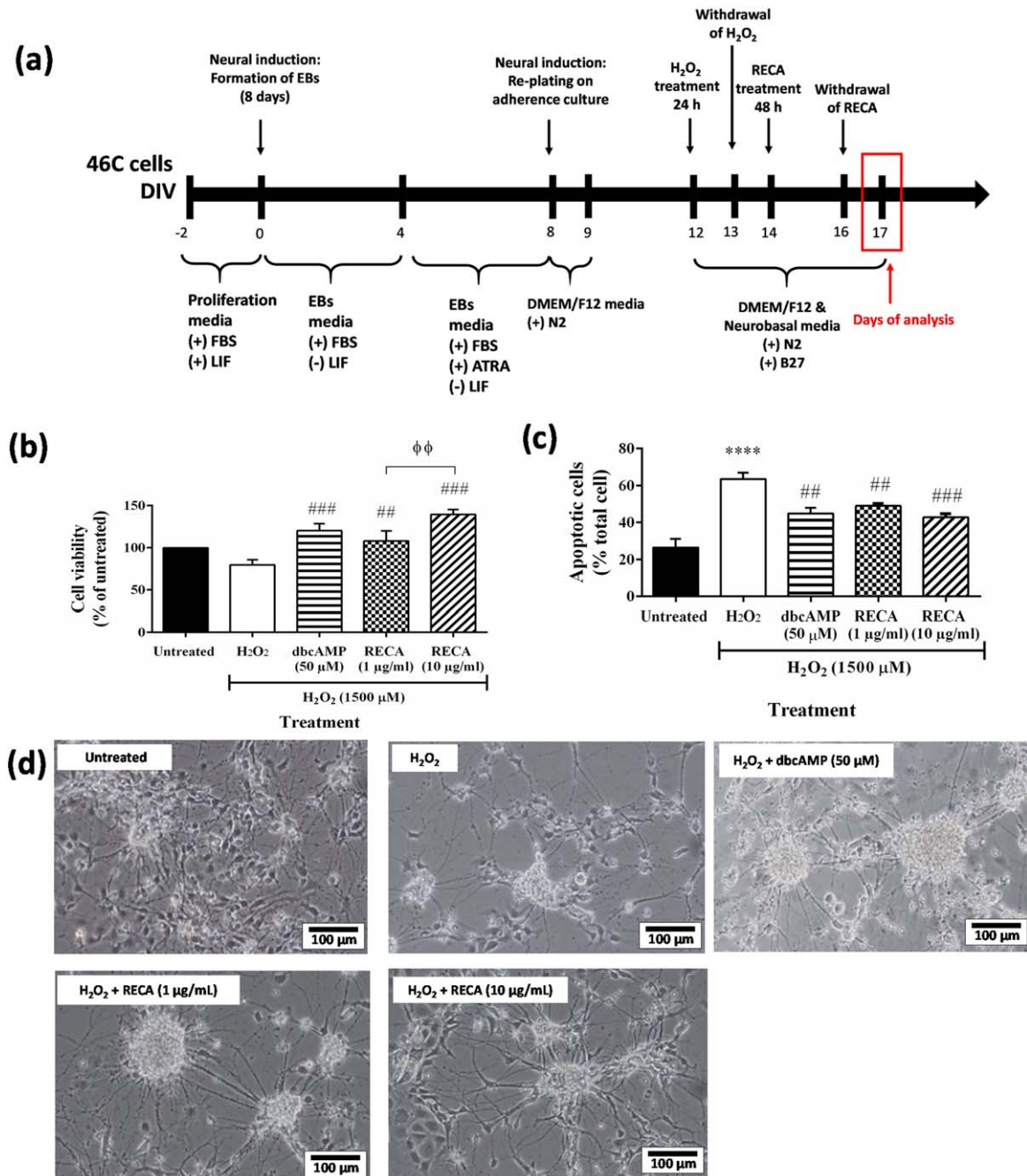


Fig. 6. Effect of post-treatment with RECA on H₂O₂-induced cytotoxicity in neural-like cells derived from 46C cells. (a) Experimental design for neuroregenerative effect of RECA in neural-like cells derived from 46C cells; (b) Percentage of cell viability. Data were expressed as the percentage of mean \pm SEM ($n = 3$), where ## indicates $p < 0.01$ and ### indicates $p < 0.001$ (significantly different from H₂O₂-treated cells); $\phi\phi$ indicates $p < 0.01$ (significantly different between the RECA-treated cells) (One way ANOVA and *post-hoc* Bonferroni's test). (c) Effect of RECA on the apoptotic rate in H₂O₂-treated 46C-derived neural-like cells. The values represent the percentage of apoptotic cells. Data represent the mean \pm SD ($n = 3$), where **** indicates $p < 0.0001$ (significantly different from untreated cells); # indicates $p < 0.05$, ## indicates $p < 0.01$, ### indicates $p < 0.001$ (significantly different from H₂O₂-treated cells) [(one-way ANOVA and *post-hoc* Bonferroni's test)]. (d) Effect of RECA on H₂O₂-induced morphological alteration in 46C-derived neural-like cells. The characteristic features of H₂O₂-induced cytotoxicity include decrease in cell number and presence of neurites degeneration. Co-treatment with RECA ameliorated the H₂O₂-induced cell damage. The scale bars represent 100 μ m for micrographs (magnification 20 \times).

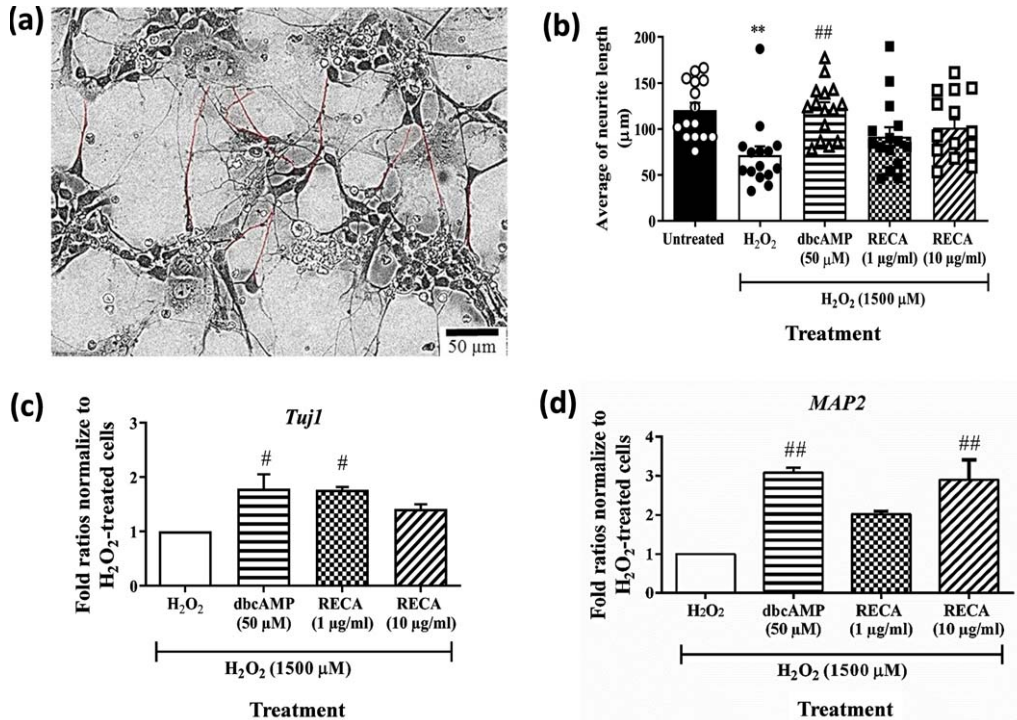


Fig. 7. Effect of RECA on the neurite outgrowth and neuronal specific markers in H₂O₂-treated 46C-derived neural-like cells treated with RECA for 48 h. (a) Neurite tracing for neurite outgrowth measurement using Neuron J (Maryland, USA), marked by red trace. (b) The bar graph represents the mean neurite length of 15 single cells from 4 - 5 random fields. The scale bars represent 50 µm for micrographs. RT-qPCR analysis of (c) *Tuj1* and (d) *MAP2* in H₂O₂-treated 46C-derived neural-like cells after RECA treatment for 48 h. Expression levels represented as fold change of treatment groups over the expression of H₂O₂-treated cells. Data represent mean ± SEM ($n = 15$ for neurite measurement; $n = 3$ for RT-qPCR analysis), where ** $p < 0.01$ (significantly different from untreated cells); # indicates $p < 0.05$ and ## indicates $p < 0.01$ (significantly different from H₂O₂-treated cells) (One way ANOVA and *post-hoc* Bonferroni test).

firmly the earlier MTT results (Fig. 6b) that RECA confers regeneration against H₂O₂-induced cell damage. The percentage of total apoptotic cells was $26.4 \pm 4.8\%$ in the untreated group of 46C-derived neural-like cells, which was significantly lower than in the H₂O₂-treated cells alone, which exhibited an apoptotic rate of $63.5 \pm 3.5\%$ ($p < 0.001$). 48 h post-treatment with 1 µg/mL and 10 µg/mL of RECA attenuated H₂O₂-induced apoptosis, $49.0 \pm 1.2\%$ ($p < 0.01$) and $42.8 \pm 2.0\%$ ($p < 0.001$), respectively, when compared to H₂O₂-treated cells alone. Meanwhile, dbcAMP reduces the severity of H₂O₂-induced cell injury by $44.9 \pm 3.2\%$ ($p < 0.01$). Nevertheless, the anti-apoptosis effect of RECA on H₂O₂-induced apoptosis was not dose-dependent in 46C-derived neural-like cells.

Effect of RECA on the neurite outgrowth in H₂O₂-treated 46C-derived neural-like cells

In this study, we examined the effects of RECA on neurite elongation in H₂O₂-treated 46C-derived neural-like cells. The dynamic changes in neurite morphology were observed in 46C-derived neural-like cells after 24 h treatment with H₂O₂. Following 48 h of treatment with RECA, it was seen that 1 and 10 µg/mL of RECA elicited abundant neurite outgrowth from the H₂O₂-treated 46C-derived neural-like cells that also appeared more flattened and adherent to the adhesive substratum (laminin) in a similar manner as observed in the undamaged neural-like cells (H₂O₂-untreated cells). The quantitative image analysis by Neuron J showed that RECA and dbcAMP dramatically increased the average length of neurites in the H₂O₂-treated neural-like cells (Fig. 7a, b). The heterogeneous morphology of neural-like cells derived from differentiated 46C EBs, including cell clumps with multiple neurite projections,

made the cell viewing uncompromising. Therefore, only the neurites extending from a single soma cell of neurons were measured. The cells appeared to demonstrate both multipolar and bipolar projections.

*Effect of RECA on the *Tuj1* and *MAP2* expression in H_2O_2 -treated 46C-derived neural-like cells*

In the post-treatment study, $1500\ \mu\text{M}$ H_2O_2 increased the degree of cell injury as indicated by decreased expression of *Tuj1* and *MAP2* in the neural-like cells treated with H_2O_2 . *Tuj1* level was found to be downregulated in H_2O_2 -treated cells. 48 h post-treatment with RECA at concentrations of 1 and $10\ \mu\text{g}/\text{mL}$ in cells that were exposed to H_2O_2 toxicity marginally increased the levels of *Tuj1* expression by 1.76-fold ($p < 0.05$) and 1.41-fold, respectively, when compared to H_2O_2 -treated cells alone (Fig. 7c). Post-treatment with dbcAMP at a concentration of $50\ \mu\text{M}$ in cells exposed to H_2O_2 toxicity significantly increased the levels of *Tuj1* expression with a percentage of 1.78-fold ($p < 0.05$), when compared to H_2O_2 -treated cells alone.

Furthermore, *MAP2* level was found to be downregulated in H_2O_2 -treated cells by 60%, when compared to untreated neural-like cells (Data not shown). Meanwhile, post-treatment with RECA at concentrations of 1 and $10\ \mu\text{g}/\text{mL}$ in cells that were exposed to H_2O_2 toxicity increased the levels of *MAP2* expression (Fig. 7d) by 2.0-fold and 2.9-fold ($p < 0.01$), when compared to H_2O_2 -treated cells alone. Post-treatment with dbcAMP at the concentration of $50\ \mu\text{M}$ in cells that were exposed to H_2O_2 toxicity also increased the levels of *MAP2* expression with fold ratios of 3.09-fold ($p < 0.01$) when compared to H_2O_2 -treated cells alone.

Effect of RECA on the intracellular ROS in H_2O_2 -induced oxidative stressed neural-like cells differentiated from 46C

To determine the effect of RECA on oxidative stress, the production of intracellular ROS was monitored by the green fluorescence of $H_2\text{DCFDA}$ using flow cytometry. Figure 8a shows that the histogram peak gradually shifted to the right when cells were treated with H_2O_2 , indicating the increase in the intensity of the green fluorescence of $H_2\text{DCFDA}$ when compared to untreated cells. The histogram peak shifted to the left compared to H_2O_2 -treated neural-like cells when the cells were incubated with RECA and dbcAMP. As shown in

Fig. 8b, exposure of 46C-derived neural-like cells to H_2O_2 significantly elevated intracellular ROS level ($45.7 \pm 3.63\%$; $p < 0.01$) compared to the untreated cells (13.4 ± 1.60 ; $p < 0.01\%$). Interestingly, the antioxidant effect of RECA on H_2O_2 -induced oxidative stress was dose-dependent in 46C-derived neural-like cells. At 48 h post-treatment with RECA (1 and $10\ \mu\text{g}/\text{mL}$), the intracellular ROS level reduced to $31.5 \pm 3.79\%$ ($p > 0.05$), and 24.3 ± 2.17 ($p < 0.05$), respectively, compared to H_2O_2 -treated neural-like cells. Insignificant reduction was also observed in treatment with the dbcAMP-treated group ($28.6 \pm 4.31\%$; $p > 0.05$).

Effect of RECA on antioxidant gene expression in H_2O_2 -treated 46C-derived neural-like cells

To evaluate the potential involvement of antioxidant enzymes in regulating apoptotic cell injury/death induced by H_2O_2 , expression of *Trx1* and *HO-1* were measured at mRNA level by RT-qPCR. A significant decrease in the expression of the *Trx1* gene was detected in H_2O_2 -treated neural-like cells (Fig. 8c). However, post-treatment with 1 and $10\ \mu\text{g}/\text{mL}$ RECA notably enhanced the expression of these antioxidant enzymes by 3.6-fold and 4.70-fold ($p < 0.05$), respectively. Post-treatment with dbcAMP at the concentration of $50\ \mu\text{M}$ in cells exposed to H_2O_2 toxicity slightly increased the levels of *Trx1* expression with fold ratios of 4.0-fold when compared to H_2O_2 -treated cells alone.

A significant decrease in the expression of the *HO-1* gene was detected in H_2O_2 -treated neural-like cells by 0.20-fold ($p < 0.01$) (Fig. 8d) when compared with H_2O_2 -untreated neural-like cells. However, post-treatment with 1 and $10\ \mu\text{g}/\text{mL}$ RECA notably enhanced the expression of these antioxidant enzymes by 4.6-fold and 7.8-fold ($p < 0.001$), respectively. Surprisingly, the increment in the *HO-1* gene did not evident in 46C-derived neural-like cells after treatment with $50\ \mu\text{M}$ dbcAMP.

DISCUSSION

In the present study, we developed H_2O_2 -induced oxidative stress associated with the AD model using neural-like cells derived from the mouse embryonic stem cell line (46C). The neurotoxicity of H_2O_2 has been well-documented in previous studies using either primary neuronal cells or immortalized cell lines, such as PC12 and SH-SY5Y neuroblastoma cells. It is suggested that stem cell lines may provide

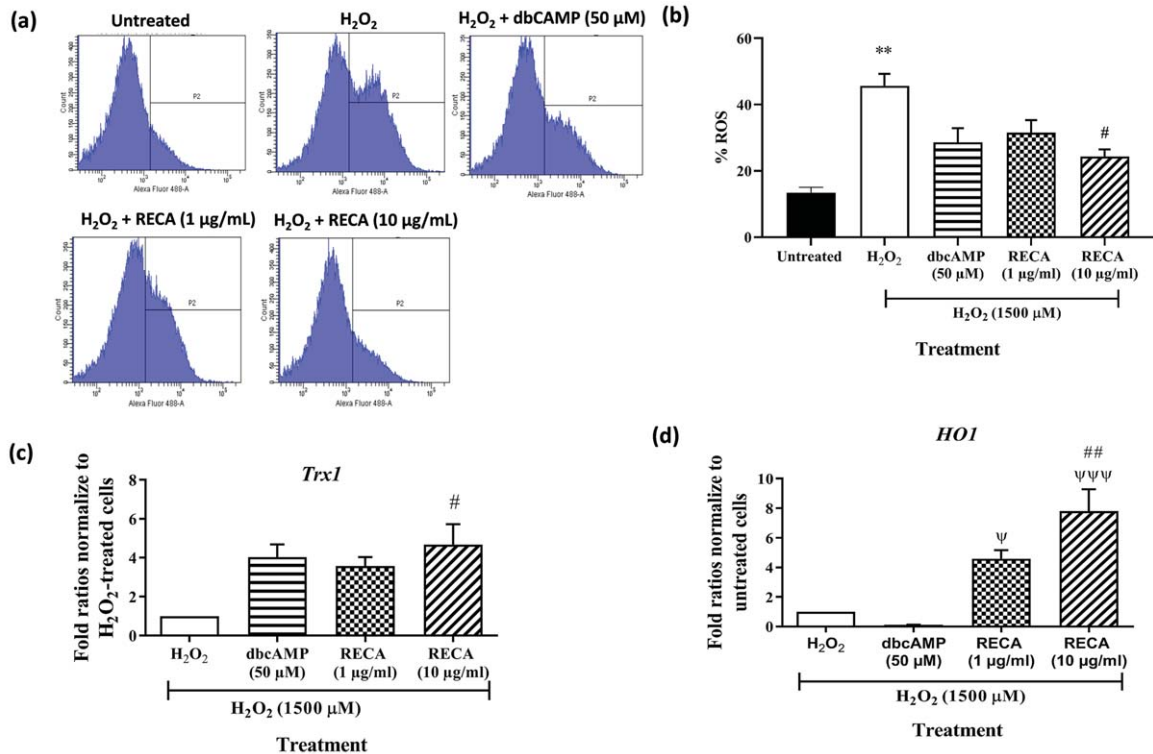


Fig. 8. (a) Intracellular ROS generation within the cells labelled with 2', 7'-dichlorodihydrofluorescein diacetate (H₂DCF-DA) was measured by flow cytometry and (b) the percentage of ROS generation was presented in the graph. RT-qPCR analysis of (c) *Trx-1* and (d) *HO-1* mRNA expression in H₂O₂-treated 46C- derived neural-like cells. β -actin was used as a housekeeping gene. Expression levels represented as fold change of treatment groups over the expression of H₂O₂-treated cells. Data are presented as mean \pm SEM ($n = 3$), where ** indicates $p < 0.01$ (vs untreated group), # indicates $p < 0.05$; and ## indicates $p < 0.001$ (significantly different from H₂O₂-treated cells), ψ indicates $p < 0.05$; $\psi\psi\psi$ indicates $p < 0.001$ (significantly different from 50 μ M dbcAMP-treated cells (One way ANOVA and *post-hoc* Bonferroni's test).

more reliable sources of neurons and glial cells as they represent a normal condition prior to the pathogenicity of AD development. In the first part of the study, the characterization of the 46C cell line was carried out based on their morphology and pluripotency status to ensure the identity and purity of our stem cells in culture. For research purposes, these characterization steps are essential and are often referred to as the gold standard before the development of neural cell profiling and disease modeling.

46C cells retain the morphology of pluripotent ES cells in the presence of LIF and on gelatin-coated as characterized by colony morphology, increased nucleus-to-cytoplasm ratio, and large nucleus with multiple nucleoli

(Fig. 2a), as well as expression of pluripotent markers such as Oct4, nanog, and Sox2 (Fig. 2b, c). LIF in our cultures, can maintain 46C cells self-renewal, signifying the activation of Janus kinase-signal transducer and activator of transcription pathway (JAK-STAT) mediated by LIF [35–36]. Gelatin is rou-

tinely used as a coating substrate for the maintenance of 46C as it has a similar molecular structure and function to collagen, thus enhancing cell attachment [37]. We also demonstrated the ability of 46C to differentiate into neuronal- and glial-like cells through the 4-/4+ protocol (Fig. 3). In our hands, 4-/4+ protocol generated neurons and neuron-supporting cells more efficiently from transgenic 46C, providing an ideal *in vitro* model that mimics an *in vivo* phenomenon, which is suitable for drug screening and brain studies. The success of the neural differentiation process of 46C was observed by the presence of a major population of Tuj1- and MAP2- positive cells, as well as a small population of CHAT- and GFAP-positive cells. Interestingly, the passage number of the 46C cell line used in this study is considered old (P25 - P40); however, this 46C cell line can maintain its pluripotency and ability to differentiate into neural cell lineage. Therefore, the 46C cell line within P25 - P40 is used in this throughout this study.

The neurogenic properties of the cell line have prompted us to test the suitability of its generated neurons as a tool to establish an *in vitro* AD model for natural product research or at least for initial screening of the neurotherapeutic potential of natural products. The *in vitro* model was previously established by treating 46C-derived neurons with H₂O₂ [25]. H₂O₂ was chosen because it has been used as the most common toxin to induce oxidative stress condition, which is the general hallmark in ND conditions, particularly in PD and AD [26–32]. In this study, two main time points need to highlight: Firstly, to determine the optimal dose of H₂O₂ to establish the AD model, the cytotoxicity and apoptosis assays were done at DIV 14. Secondly, to demonstrate the effects of RECA on the AD *in vitro* model, the cytotoxicity, apoptosis, and ROS assays, as well as RT-qPCR and neurite measurement, were done at DIV 17.

Based on cytotoxicity assay using MTT to establish *in vitro* AD model, a high concentration of H₂O₂ (1500 μM) was chosen (Fig. 4a). Our previous and present data showed a significant increase in ROS activity [25] and apoptotic rate (Fig. 4c, d) when the neural-like cells were treated with H₂O₂ at this concentration, indicating a successful establishment of an *in vitro* AD model using 46C cells by stimulating the production of ROS. Our findings agreed with Jalil and co-workers, who developed *in vitro* ND model by glutamate-induced oxidative stress in 46C-derived neuronal cells [38]. These findings demonstrate that the stem cell line could serve as an ideal *in vitro* model that mimics the AD phenomenon *in vivo*.

Some recent evidence showed that H₂O₂ could induce cell death in hippocampal neurons [39], PC12 cells [40], and SH-SY5Y cells [41], and that ROS are involved in the apoptotic mechanism of H₂O₂-mediated neurotoxicity. From our previous work, we observed that 24 h pre-treatment of 46C-derived neural-like cells with H₂O₂ resulted in suppression of cell viability in a dose-dependent manner [25]. We found that 1500 μM H₂O₂ reduced the viability of 46C-derived neural-like cells by approximately 50% (Fig. 4a) and increased the rate of apoptosis (Fig. 4d). The present study further investigated whether RECA has protective and regenerative effects against H₂O₂-induced cell death. The exposure of 1 μg/mL and 10 μg/mL of RECA for 48 h remarkably attenuated cell death by increasing the cell viability, indicating that RECA significantly prevented cell damage and death. Through phase contrast microscopy analysis, our results confirmed that in 46C-derived neural-like cells, H₂O₂ was observed to induce cell injury and

subsequent death by damaging the neuritic branches which resulted in low cell viability. In contrast, 48 h post-treatment with RECA markedly mitigated these distinct morphological changes. dbcAMP, a membrane-permeable cAMP analog was used in this study to serve as the positive control. Previous studies have shown that dbcAMP induces neurite outgrowth in neuronal cells such as PC12 [42] and N2a cell lines [43].

Interestingly, our results showed that treatment of damaged 46C-neural-like cells with RECA at concentrations 1 and 10 μg/mL restored the survival of neurons (Fig. 6) and promoted neurite extension (Fig. 7). Slower morphological changes were observed in H₂O₂-treated neural-like cells, whereas the neurotrophic effects of RECA were observed to be rapid. 48 h post-treatment with RECA resulted in cells with obvious neuronal morphology with long, extensively branched neurites. The morphology of 46C-derived neural-like cells was observed to be thick and dense, which made viewing the cells harder. Due to this problem, the number of neurites could not be determined and the measurement of neurite length was only up to 48 h post-treatment.

Although the downstream signaling mechanisms of action in this stem cell-derived neural-like cells are not fully understood, there are several possible reasons which may be the cause of neurite outgrowth of the 46C-derived neural-like cells upon treatment with RECA: 1) the antioxidant components in RECA may significantly delay or reduce the oxidation event in the damaged neurons—this concept could be exemplified by remarkable extensions of neurites via the expression of antioxidant genes after the neurons had undergone severe damage; or 2) the neurotogenic effect of RECA which has been reported to promote neurogenesis, neuronal differentiation and neurite outgrowth [17, 44, 45].

Soumyanath and co-workers reported the potential of asiatic acid in promoting *in vitro* neurite outgrowth of damaged neurons by the mitogen-activated protein (MAP) kinase pathway [17]. This finding is in good agreement with another study conducted by Wanakhachornkrai et al., who reported the neurite outgrowth in human neuroblastoma cells after 6 h treatment with standardized extract of *C. asiatica* (Eca 233) (1, 10, and 100 μg/mL) by activation of MEK/ERK and PI3K/Akt signaling pathways [44]. Furthermore, *C. asiatica* was observed to have the ability to restore cell survival and protect neurons from damage after treatment with 1-buthionine-(S,R)-sulfoximine (BSO) by increasing

cell viability and decreasing cell apoptosis. They found that *C. asiatica* significantly reduced caspase-9 activity, an apoptotic signaling pathway [46]. Apoptotic cells were detected using flow cytometry, and the present data revealed that the percentage of cells which undergo apoptosis was significantly increased in H₂O₂-pre-treated 46C-neural-like cells compared to the untreated group. 48 h post-treatment with RECA ameliorated H₂O₂-induced apoptosis in 46C-derived neural-like cells. These results are consistent with Omar and co-workers, who demonstrated that post-treatment of *C. asiatica* significantly reduced the number of apoptotic cells induced by BSO [46].

Nevertheless, we were very keen to investigate the possible cause of RECA in stimulating neurite outgrowth of the 46C-derived neural-like cells based on the expression of class III β -tubulin (*Tuj1*), *MAP2*, and antioxidant genes. *Tuj1* expression was significantly decreased after treatment with H₂O₂. This study showed that neuronal damage and loss after treatment with H₂O₂ might contribute to the downregulation of *Tuj1* expression in 46C-derived neural-like cells. *Tuj1* is expressed in newly generated immature post-mitotic neurons and differentiated neurons [47, 48]. Immunohistochemical detection is often used to study dendritic, and axonal regeneration as the protein is found in the cell bodies, dendrites, axons, and axonal terminations of post-mitotic neurons [49]. The expression of *Tuj1* is regulated in the presence of nerve growth factor [50]. The results revealed that *Tuj1* expression was upregulated in RECA- and dbcAMP-treated cells in 46C-derived neural-like cells (Fig. 7c). There are two possible reasons why insignificant increments in *Tuj1* expression were observed after treatment with RECA at 10 μ g/kg: First, low *Tuj1* expression may reflect the decreased number of post-mitotic cells in our culture; given that these neurons were in DIV 17 during the analysis, these neurons could be considered mature and committed neurons. Second, RECA might have the potential to enhance the maturation of neurons, increasing the proportion of *MAP2*-positive cells in the culture.

Further investigation revealed that the expression of matured neurons, *MAP2*, was significantly decreased in H₂O₂-treated 46c-derived neural-like cells (Fig. 7d). The selection of *MAP2* was based on the fact that this mature neuronal marker is largely localized in a somatodendritic compartment in CNS, which plays a major role in regulating axonal and dendritic morphogenesis in the nervous sys-

tem [51]. Inhibition of *MAP2* expression has been reported to interfere with neuronal migration, dendritic outgrowth, and microtubule organization in *MAP2/MAP1B* knockout mice [52]. The expression of *MAP2* is regulated in the presence of nerve growth factor [53, 54], dbcAMP [55], and retinoic acid [56]. *MAP2* expression was upregulated in H₂O₂-treated neural-like cells after treatment with 1 μ g/mL of RECA, and significantly upregulated after treatment with 10 μ g/mL of RECA compared to H₂O₂-treated neural-like cells alone. The higher *MAP2* expression could be seen in dbcAMP-treated cells. The elevation in *MAP2* expression could therefore reflect an increase in the growth of the neurites, suggesting that RECA promotes neuritic regeneration by targeting *MAP2* expression in H₂O₂-treated 46C-derived neural-like cells, resulting in the restoration of neuronal structure and function after injury. Therefore, it is suggested that the neurogenic potential of RECA induces the regulation of *MAP2* mRNA level, ultimately promoting neurite outgrowth in 46C-derived neurons. These discoveries suggest that RECA plays a vital role in neuronal differentiation and maturation, particularly in cultured 46C-derived neural-like cells.

H₂O₂ has been reported to induce ROS generation, leading to peroxidation of membrane lipid and cellular integrity, subsequently, cell apoptosis. Previous work reported that the exposure of 46C-derived neural-like cells to H₂O₂ elevated intracellular ROS levels as compared to the untreated cells. We further looked at the role of *Trx1* and *HO-1* genes in H₂O₂-induced oxidative stress in 46C-derived neural-like cells. *Trx1* and *HO-1*, are anti-oxidative enzymes responsive to oxidative stress. In particular, the change in *Trx1* expression during H₂O₂-induced cellular damage/death was evaluated. Post-treatment with 1500 μ M H₂O₂ reduces the expression of *Trx1* at the gene levels of neural-like cells from 46C (Fig. 8c). This downregulation leads to the apoptosis of neural-like cells, due to the increase in the intracellular ROS generation. *Trx1* (~12 kDa), a cytosolic ubiquitous protein, has been shown to scavenge singlet oxygen, hydroxyl radicals, and H₂O₂ [57]. *Trx* acts as an antioxidant itself [58] and as a regulator in other antioxidant pathways [59]. *Trx* is extremely vulnerable to ROS-induced oxidative stress as ROS could rapidly activate the translocation of *Trx* into the nucleus [60]. *Trx* is crucial for cell survival [61]. It is suggested that the downregulation of *Trx1* expression in neural-like cells might be involved in the activation of ROS-induced cell apoptosis via the MAPK pathway [62] in response to H₂O₂. The expression

of *Trx1* in damaged 46C-derived neural-like cells was increased upon treatment with 1 and 10 $\mu\text{g/mL}$ RECA and restored to normal expression as untreated cells. It is suggested that the antioxidant properties of RECA diminished the oxidation of *Trx1* by suppressing ROS production, leading to the restoration of cell viability and the prevention of oxidative stress-induced apoptosis. Treatment with 50 μM dbcAMP also exerted the antioxidant effect on 46C-derived neural-like cells, by upregulation *Trx1* expression.

HO-1 (~32 kDa) is a member of the stress protein superfamily that catalyzes the oxidation of heme to biliverdin in most tissues, including the brain. In response to oxidative stress insult, transcriptional upregulation of the HO-1 gene may protect the cells by stimulating the breakdown of heme to bilirubin and biliverdin [63–65], as well as regulating anti-inflammatory [66, 67], antioxidant [68], and anti-apoptotic pathway [69, 70]. Generally, the expression of *HO-1* has been observed to be activated under oxidative stress, which protects cells from cellular injury and death [65, 71, 72]. Recent studies suggest that Trx may also contribute to the upregulation of HO-1 activity associated with oxidative stress and inflammation [59, 73]. Therefore, it is postulated that the downregulation of *Trx1* expression might induce the upregulation of *HO-1* expression in these *in vitro* models. Our study showed a significant decrease in the expression of the HO-1 gene in H_2O_2 -treated 46C-derived neural-like cells, suggesting a failure in the protective role of the HO system against *in vitro* oxidative stress model. We also suspect defense mechanism through other antioxidants of the embryonic stem cells could have overtaken the activation of *HO-1* at the initial stage. Then, treatment with 1 $\mu\text{g/mL}$ and 10 $\mu\text{g/mL}$ of RECA in H_2O_2 -treated 46C-derived neural-like cells must have given alternative options to the cells to activate the HO-1 pathway. Considering the significant overexpression in *HO-1* after treatment with 10 $\mu\text{g/mL}$ RECA, it is speculated that the activity of the HO-1 in 46C-derived neural-like cells exceeded the demands for scavenging free radicals-induced oxidative stress. Therefore, RECA could play an antioxidant role through the increase in *HO-1* level which may be acting as an efficient ROS scavenger. It is worth noting that activation of defense mechanisms by other antioxidants such as N-acetyl-L-cysteine and mitochondria-targeted ubiquinone (MitoQ) in the cells should be assessed in the future [74]. These findings were in good agreement with Sasmita and co-workers who demonstrated the anti-inflammatory

effect of Madecassoside, a triterpene of CA in lipopolysaccharide-induced microglia via the upregulation of HO-1 gene expression [75]. Interestingly, no significant difference in the expression of HO-1 gene when treated with dbcAMP in this cell model, suggesting that the intracellular ROS accumulation was not attenuated by the treatment of dbcAMP.

Together, these findings suggest that the increase in endogenous antioxidant levels might be a possible mechanism involved in the neuroregenerative effect of RECA in decreasing the intracellular ROS level, regulating cell survival and neurite outgrowth, as well as preventing cell apoptosis. Therefore, these results revealed that the bioactive compounds in CA have potent antioxidant properties which could be useful as the adjunct treatment for oxidative stress associated-ND. These results are in good agreement with a previous study demonstrating that CA and its derivatives better protect cells against oxidative stress-induced apoptosis and promote neurite outgrowth in other cell lines, including SH-SY5Y [44, 46]. Although the present study has shown that RECA has neuroregenerative effects on neural-like cells, further studies are needed to study the mechanism of actions of how this herb can exert therapeutic effects in our 46C-derived neural-like cells model. Furthermore, the current study indicates that neural-like cells differentiate from stem cells may be efficiently suitable to be used for the establishment of neurodegenerative model associated with oxidative stress, suitable for drug screening and fundamental studies. These results parallel to the findings from the study conducted by Jalil and co-workers, who established the oxidative stress model using 46C-derived neuronal cells treated with glutamate-induced excitotoxicity [38]. Therefore, neural-like cells derived from animal stem cells, such as mouse ES stem cell provides important fundamental knowledge of the AD model and will help guide future studies using this stem cell for the development of AD drugs. Figure 9 illustrates the proposed RECA mechanism of action as the potential treatment for AD mitigating oxidative stress.

Conclusion

Our findings highlight the effect of RECA in reducing the intracellular ROS activity in H_2O_2 -damaged stem cell-derived neurons, thus increasing the viability of these neurons. Interestingly, neurite outgrowth of these neurons was observed to be remarkably improved upon treatment with RECA, with increased

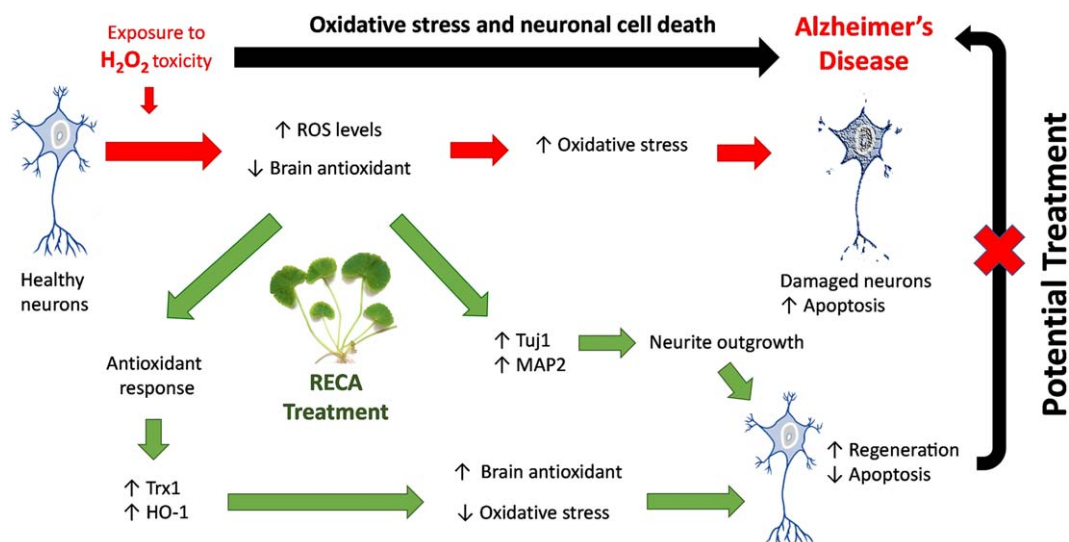


Fig. 9. Mechanism of action of RECA as the potential treatment for AD by mitigating oxidative stress. RECA promotes increased expression of antioxidant enzyme genes (i.e., *Trx1* and *HO-1*) to compensate for antioxidant response to oxidative toxicity (i.e., H_2O_2). RECA-mediated attenuation of increased ROS in neurons, results in reduced oxidative stress, leading to the restoration of cell viability and the prevention of oxidative stress-induced apoptosis. In addition, RECA promotes neuritic regeneration by modulating *Tuj1* and *MAP2* genes expression, resulting in the restoration of neuronal structure and function after injury. These potential mechanisms are proposed to be the underlying basis for the restoration of neuronal function and structure after injury demonstrated in oxidative stress-induced AD treated with RECA.

expression of neuronal protein markers, particularly MAP2, and antioxidant genes, particularly *Trx1* and *HO-1*. Based on these results, we postulate RECA to exert its neuroregenerative effect prospectively by targeting MAP2 expression and acting as an efficient ROS scavenger in restoring cell viability and preventing oxidative stress-induced apoptosis. The use of standardized raw extract in this study undoubtedly indicates the synergistic activity of RECA phytochemical constituents in promoting neuroregeneration. We conclude that RECA has many potentials that are worth exploring, particularly in unraveling the active compound(s) involved and the mode of action of its neuroprotective and neuroregenerative capabilities in *in vitro* AD-associated with oxidative stress model.

ACKNOWLEDGMENTS

The authors sincerely thank Professor Dr. John Orr Mason (University of Edinburgh, Scotland, UK) for providing 46C cell line, and Professor Dr. Mohd Ilham Adenan (Universiti Teknologi Malaysia, Selangor, Malaysia) for providing standardized RECA. The authors also thank the colleagues in the Stem Cell Research Lab and Medical Genetics Lab, Faculty of Medicine and Health Science, UPM, Malaysia.

FUNDING

This work was supported by the Ministry of Agriculture of Malaysia (MOA) through NKEA Research Grant Scheme (NRGS) [Project number: NH1014D045] awarded to NN. NIM is a recipient of the Graduate Research Fellowship (GRF), Universiti Putra Malaysia (UPM).

CONFLICT OF INTEREST

The authors declared no conflict of interest.

DATA AVAILABILITY

The data supporting the findings of this study are available on request from the corresponding author. The data are not publicly available due to privacy or ethical restrictions.

REFERENCES

- [1] Rao KGM, Rao SM, Rao SG (2006) *Centella asiatica* (L.) Leaf extract treatment during the growth spurt period enhances hippocampal ca_3 neuronal dendritic arborization in rats. *eCAM* 3, 349-357.
- [2] Maulidiani, Abas F, Khatib A, Perumal V, Suppaiah V, Ismail A, Hamid M, Shaari K, Lajis NH (2016) Metabolic alteration in obese diabetes rats upon treatment with Cen-

- tella asiatica extract. *J Ethnopharmacol* **180**, 60-69.
- [3] Zainol M, Abd-Hamid A, Yusof S, Muse R (2003) Antioxidative activity and total phenolic compounds of leaf, root and petiole of four accessions of *Centella asiatica* (L) Urban. *Food Chem* **81**, 575-581.
- [4] Qi F, Yang L, Tian Z, Zhao M, Liu S, An J (2014) Neuroprotective effects of Asiaticoside. *Neural Regen Res* **9**, 1275-1282.
- [5] Zhang X, Wu J, Dou Y, Xia B, Rong W, Rimbach G, Lou Y (2012) Asiatic acid protects primary neurons against C2-ceramide-induced apoptosis. *Eur J Pharmacol* **679**, 51-59.
- [6] Schaneberg B, Mikell J, Bedir E, Khan IA (2003) An improved HPLC method for quantitative determination of six triterpenes in *Centella asiatica* extracts and commercial products. *Pharmazie* **58**, 381-384.
- [7] Somboonwong J, Kankaisre M, Tantisira B, Tantisira MH (2012) Wound healing activities of different extracts of *Centella asiatica* in incision and burn wound models: An experimental animal study. *BMC Complement Altern Med* **12**, 1-7.
- [8] Shetty BS, Udupa SL, Udupa AL, Somayaji SN (2006) Effect of *Centella asiatica* L (Umbelliferae) on normal and dexamethasone-suppressed wound healing in Wistar albino rats. *Int J Low Extrem Wounds* **5**, 137-143.
- [9] Azis HA, Taher M, Ahmed AS, Sulaiman WMAW, Susanti D, Chowdhury SR, Zakaria ZA (2017) *In vitro* and *in vivo* wound healing studies of methanolic fraction of *Centella asiatica* extract. *S Afr J Bot* **108**, 163-174.
- [10] Wanasuntronwong A, Tantisira MH, Tantisira B, Watanabe H (2012) Anxiolytic effects of standardized extract of *Centella asiatica* (ECa 233) after chronic immobilization stress in mice. *J Ethnopharmacol* **143**, 579-585.
- [11] Kalshetty P, Aswar U, Bodhankar S, Sinnathambi A, Mohan V, Thakurdesai P (2012) Antidepressant effects of standardized extract of *Centella asiatica* L in olfactory bulbectomy model. *J Ethnopharmacol* **2**, 48-53.
- [12] Jagadeesan S, Chiroma MS, Baharuldin MTH, Taib CNM, Amom Z, Adenan MI, Moklas MAM (2019). *Centella asiatica* prevents chronic unpredictable mild stress-induced behavioral changes in rats. *Biomed Res Ther* **6**, 3233-3243.
- [13] Kumar, MHV, Gupta, YK (2002) Effect of different extracts of *Centella asiatica* on cognition and markers of oxidative stress in rats. *J Ethnopharmacol* **79**, 253-260.
- [14] Gupta, YK, Kumar MHV, Srivastava, AK (2003) Effect of *Centella asiatica* on pentylentetrazole-induced kindling, cognition and oxidative stress in rats. *Pharmacol Biochem Behav* **74**, 579-585.
- [15] Rosdah AA, Lusiana E, Reagan M, Akib A, Khairunnisa F, Husna A (2018) Enhancing cognitive function of healthy wistar rats with aqueous extract of *Centella asiatica*. *Acta Biochim Indonesia* **1**, 37-45.
- [16] Rao SB, Chetana M, Devi PU (2005) *Centella asiatica* treatment during postnatal period enhances learning and memory in mice. *Physiol Behav*, **86**, 449-457.
- [17] Soumyanath A, Zhong Y, Gold SA, Yu X, Koop DR, Bourdette D, Gold BG (2005) *Centella asiatica* accelerates nerve regeneration upon oral administration and contains multiple active fractions increasing neurite elongation *in-vitro*. *J Pharm Pharmacol* **57**, 1221-1229.
- [18] Jiang H, Zheng G, Lv J, Chen H, Lin J, Li Y, Fan G, Ding X (2016) Identification of *Centella asiatica*'s effective ingredients for inducing the neuronal differentiation. *Evid Based Complement Alternat Med* **2016**, 9634750.
- [19] Chiroma SM, Baharuldin MTH, Taib CNM, Amom Z, Jagadeesan S, Adenan MI, Moklas MAM (2019) Protective effect of *Centella asiatica* against D-galactose and aluminium chloride induced rats: Behavioral and ultrastructural approaches. *Biomed Pharmacother* **109**, 853-864.
- [20] Gray NE, Harris CJ, Quinn JF, Soumyanath A (2016) *Centella asiatica* modulates antioxidant and mitochondrial pathways and improves cognitive function in mice. *J Ethnopharmacol* **180**, 78-86.
- [21] Hafiz ZZ, Shamsuddin N, Mukhtar SM, James RJ, Adenan MI (2018) Anti-acetylcholinesterase, anti-inflammatory and anti-oxidant activities of raw-extract centella asiatica (reca) on lipopolysaccharide (LPS)-induced neuroinflammation Sprague Dawley rats. *Int J Eng Technol* **7**, 96-101.
- [22] Hafiz ZZ, Amin M, 'Afif M, James RMJ, Teh LK, Salleh MZ, Adenan MI (2020) Inhibitory effects of raw-extract *Centella asiatica* (RECA) on acetylcholinesterase, inflammations, and oxidative stress activities via *in vitro* and *in vivo*. *Molecules* **25**, 1-20.
- [23] Lu P, Jones L, Snyder EY, Tuszyński MH (2003) Neural stem cells constitutively secrete neurotrophic factors and promote extensive host axonal growth after spinal cord injury. *Exp Neurol* **181**, 115-129.
- [24] Aubert J, Stavridis MP, Tweedie S, Reilly MO, Vierlinger K, Li M, Ghazal P, Pratt T, Mason JO, Roy D, Smith A (2003) Screening for mammalian neural genes via fluorescence-activated cell sorter purification of neural precursors from Sox1- gfp knock-in mice. *Proc Natl Acad Sci U S A* **100**(Suppl 1), 11836-11841
- [25] Mansor NI, Azmi N, Ling K, Rosli R, Hassan Z, Nordin N (2019) Prospective stem cell lines as *in vitro* neurodegenerative disease models for natural product research. *Neurosci Res Notes* **2**, 16-30.
- [26] Lennicke C, Rahn J, Lichtenfels R, Wessjohann LA, Seliger B (2015) Hydrogen peroxide - production, fate and role in redox signaling of tumor cells. *Cell Commun Signal* **13**, 1-19.
- [27] Yang J, Yang J, Liang SH, Xu Y, Moore A, Ran C (2016) Imaging hydrogen peroxide in Alzheimer's disease via cascade signal amplification. *Sci Rep* **6**, 35613.
- [28] Tabner BJ, El-Agnaf OM, Turnbull S, German MJ, Paleologou KE, Hayashi Y, Cooper LJ, Fullwood NJ, Allsop D (2005) Hydrogen peroxide is generated during the very early stages of aggregation of the amyloid peptides implicated in Alzheimer disease and familial British dementia. *J Biol Chem* **280**, 35789-35792.
- [29] Su XY, Wu WH, Huang ZP, Hu J, Lei P, Yu CH, Zhao YF, Li YM. Hydrogen peroxide can be generated by tau in the presence of Cu(II). *Biochem Biophys Res Commun* **358**, 661-665.
- [30] Singh M, Sharma, H, Singh N (2007) Hydrogen peroxide induces apoptosis in HeLa cells through mitochondrial pathway. *Mitochondrion* **7**, 367-373.
- [31] Tartier, L, Mccarey, YL, Biaglow, JE, Kochevar, IE (2000) Apoptosis induced by dithiothreitol in HL-60 cells shows early activation of caspase 3 and is independent of mitochondria. *Cell Death Differ* **7**, 1002-1010.
- [32] Lee JE, Sohn J, Lee JH, Lee KC (2000) Regulation of bcl-2 family in hydrogen peroxide-induced apoptosis in human leukemia HL-60 cells. *Exp Mol Med* **32**, 42-46.
- [33] Omar N, Lokanathan Y, Razi ZRM, Idrus R (2019) The effects of *Centella asiatica* (L) Urban on neural differentiation of human mesenchymal stem cells *in vitro*. *BMC Complement Alternat Med* **19**, 167.

- [34] Kim KM, Son K, Palmore G (2015) Neuron Image Analyzer: Automated and accurate extraction of neuronal data from low quality images. *Sci Rep* **5**, 17062.
- [35] Ohtsuka S, Nakai-futatsugi Y, Niwa H (2015) LIF signal in mouse embryonic stem cells. *JAKSTAT* **4**, e1086520.
- [36] Onishi K, Zandstra PW (2015) LIF signaling in stem cells and development. *Development* **142**, 2230-2236.
- [37] Bello AB, Kim D, Kim D, Park H, Lee SH (2020) Engineering and functionalization of gelatin biomaterials: From cell culture to medical applications. *Tissue Eng Part B Rev* **26**, 164-180.
- [38] Jalil AA, Khaza H, Nordin N, Mansor N, Zaulkffali AS (2017) Vitamin E-mediated modulation of glutamate receptor expression in an oxidative stress model of neural-like cells derived from embryonic stem cell cultures. *Evid Based Complement Alternat Med* **2017**, 6048936.
- [39] Chen X, Zhang Q, Cheng Q, Ding F (2009) Protective effect of salidroside against H₂O₂-induced cell apoptosis in primary culture of rat hippocampal neurons. *Mol Cell Biochem* **332**, 85-93.
- [40] Jang J, Surh Y (2001) Protective effects of resveratrol on hydrogen peroxide-induced apoptosis in rat pheochromocytoma (PC12) cells. *Mutat Res* **496**, 181-190.
- [41] Zhang L, Yu H, Sun, Y, Lin X, Chen B, Tan C, Cao G, Wang, Z (2007) Protective effects of salidroside on hydrogen peroxide-induced apoptosis in SH-SY5Y human neuroblastoma cells. *Eur J Pharmacol* **564**, 18-25.
- [42] Maruoka H, Sasaya H, Shimamura Y, Nakatani Y, Shimoke K, Ikeuchi T (2010) Dibutyl-*c*-AMP up-regulates *nur77* expression via histone modification during neurite outgrowth in PC12 cells. *J Biochem* **148**, 93-101.
- [43] Tremblay RG, Sikorska M, Sandhu JK, Lanthier P, Ribocco-Lutkiewicz M, Bani-Yaghoub M (2010) Differentiation of mouse Neuro 2A cells into dopamine neurons. *J Neurosci Methods* **186**, 60-67.
- [44] Wanakhachornkrai O, Pongrakhananon V, Chunhacha P, Wanasuntronwong A, Vattanajun A, Tantisira B, Chanvorachote P, Tantisira MH (2013) Neuritogenic effect of standardized extract of *Centella asiatica* ECa233 on human neuroblastoma cells. *BMC Complement Altern Med* **13**, 204.
- [45] Kim H, Hong JT, Park MH (2015) *Centella asiatica* enhances neurogenesis and protects neuronal cells against H₂O₂-induced oxidative injury. *J Biomed Res* **16**, 121-128.
- [46] Omar NS, Akmal Z, Zakaria, C, Mian TS (2011) *Centella asiatica* modulates neuron cell survival by altering caspase-9 pathway. *J Med Plant Res* **5**, 2201-2209.
- [47] Von Bohlen Und Halbach O (2007) Immunohistological markers for staging neurogenesis in adult hippocampus. *Cell Tissue Res* **329**, 409-420.
- [48] Gould E, Vail N, Wagers M, Gross CG (2001) Adult-generated hippocampal and neocortical neurons in macaques have a transient existence. *Proc Natl Acad Sci U S A* **98**, 10910-10917.
- [49] Tanapat P (2013) Neuronal cell markers. *Mater Method* **3**, 196.
- [50] Yan X, Wang S, Yu A, Shen X, Zheng H, Wang L (2019) Cell chromatography-based screening of the active components in Buyang Huanwu decoction promoting axonal regeneration. *Biomed Res Int* **2019**, 6970198.
- [51] Iwata M, Muneoka KT, Shirayama Y, Yamamoto A, Kawahara R (2005) A study of a dendritic marker, microtubule-associated protein 2 (MAP-2), in rats neonatally treated neurosteroids, pregnenolone and dehydroepiandrosterone (DHEA). *Neurosci Lett* **386**, 145-149.
- [52] Teng J, Takei Y, Harada A, Nakata T, Chen J Hirokawa, N (2001) Synergistic effects of MAP2 and MAP1B knockout in neuronal migration, dendritic outgrowth, and microtubule organization. *J Cell Biol* **155**, 65-76.
- [53] Fontaine-Lenoir V, Chambraud B, Fellous A, David S, Duchossoy Y, Baulieu EE, Robel P (2006) Microtubule-associated protein 2 (MAP2) is a neurosteroid receptor. *Proc Natl Acad Sci U S A* **103**, 4711-4716.
- [54] Kristiansen M, Menghi F, Hughes R. Hubank M, Ham J (2011) Global analysis of gene expression in NGF-deprived sympathetic neurons identifies molecular pathways associated with cell death. *BMC Genomics* **12**, 551.
- [55] Zhou Y, Wu S, Liang C, Lin Y, Zou Y, Li K, Lu B, Shu M, Huang Y, Zhu W, Kang Z, Xu D, Hu J, Yan G (2015) Transcriptional upregulation of microtubule-associated protein 2 is involved in the protein kinase A-induced decrease in the invasiveness of glioma cells. *Neuro Oncol* **17**, 1578-1588.
- [56] Yu S, Levi L, Siegel R, Noy N (2012) Retinoic acid induces neurogenesis by activating both retinoic acid receptors (RARs) and peroxisome proliferator-activated receptor β/δ (PPAR β/δ). *J Biol Chem* **287**, 42195-42205.
- [57] Stroeve S, Tyul E, Glushchenko T, Tugoi I, Samoilo V, Pelto-Huikko M (2009) Thioredoxin-1 expression levels in rat hippocampal neurons in moderate hypobaric hypoxia. *Neurosci Behav Physiol* **39**, 1-5.
- [58] Das KC, Das CK (2000) Thioredoxin, a singlet oxygen quencher and hydroxyl radical scavenger: Redox independent functions. *Biochem Biophys Res Commun* **277**, 443-447.
- [59] Wiesel P, Foster LC, Pellacani A, Layne MD, Hsieh CM, Huggins GS, Strauss P, Yet SF, Perrella MA (2000) Thioredoxin facilitates the induction of heme oxygenase-1 in response to inflammatory mediators. *J Biol Chem* **275**, 24840-24846.
- [60] Go YM, Jones DP (2010) Redox control systems in the nucleus: Mechanisms and functions. *Antioxid Redox Signal* **13**, 489-509.
- [61] Mochizuki M, Kwon Y, Yodoi J, Masutani H (2009) Thioredoxin regulates cell cycle via the ERK1/2-Cyclin D1 pathway. *Antioxid Redox Signaling* **11**, 2957-2971.
- [62] Huh KH, Cho Y, Kim BS, Do, JH, Park Y, Joo DJ, Kim MS, Kim YS (2013) The role of thioredoxin 1 in the mycophenolic acid-induced apoptosis of insulin-producing cells. *Cell Death Dis* **4**, e721.
- [63] Chen K, Gunter K, Maines MD (2000) Neurons overexpressing heme oxygenase-1 resist oxidative stress-mediated cell death. *J Neurochem* **75**, 304-313.
- [64] Gozzelino R, Jeney V, Soares MP (2010) Mechanisms of cell protection by heme oxygenase-1. *Annu Rev Pharmacol Toxicol* **50**, 323-354.
- [65] Schipper HM (2000) Heme oxygenase-1: Role in brain aging and neurodegeneration. *Exp Gerontol* **35**, 821-830.
- [66] Maeda S, Nakatsuka I, Hayashi Y, Higuchi H, Shimada M, Miyawaki T (2008) Heme oxygenase-1 induction in the brain during lipopolysaccharide-induced acute inflammation. *Neuropsychiatr Dis Treat* **4**, 663-667.
- [67] Chora AA, Fontoura P, Cunha A, Pais TF, Cardoso S, Ho PP, Lee LY, Sobel RA, Steinman L, Soares MP (2007) Heme oxygenase-1 and carbon monoxide suppress autoimmune neuroinflammation. *J Clin Invest* **117**, 438-447.
- [68] Parfenova H, Leffler CW, Basuroy S Liu, J (2012) Antioxidant roles of heme oxygenase, carbon monoxide, and bilirubin in cerebral circulation during seizures. *J Cerebr Blood Flow Metab* **32**, 1024-1034.

- [69] Silva G, Cunha A, Grégoire IP, Seldon MP, Soares MP (2015) The antiapoptotic effect of heme oxygenase-1 in endothelial cells involves the degradation of p38 α MAPK isoform. *J Immunol* **177**, 1894-1903.
- [70] Fang J, Akaike T, Maeda H (2004) Antiapoptotic role of heme oxygenase (HO) and the potential of HO as a target in anticancer treatment. *Apoptosis* **9**, 27-35
- [71] Poon HF, Calabrese V, Scapagnini G Butterfield DA (2004) Free radicals: Key to brain aging and heme oxygenase as a cellular response to oxidative stress. *J Gerontol* **59**, 478-493.
- [72] Ryter SW, Choi AMK (2002) Heme oxygenase-1: Molecular mechanisms of gene expression in oxygen-related stress. *Antioxid Redox Signal* **4**, 625-632.
- [73] Koneru S, Penumathsa SV, Thirunavukkarasu M, Zhan, L Maulik N (2009) Thioredoxin-1 gene delivery induces heme oxygenase-1 mediated myocardial preservation after chronic infarction in hypertensive rats. *Am J Hypertens* **22**, 183-190.
- [74] Lee J, Cho YS, Jung H, Choi I (2018) Pharmacological regulation of oxidative stress in stem cells. *Oxid Med Cell Longev* **2018**, 4081890.
- [75] Sasmita AO, Pick A, Ling K, Gah K, Voon L, Koh R Y, Wong YPEI (2018) Madecassoside activates anti-neuroinflammatory mechanisms by inhibiting lipopolysaccharide-induced microglial inflammation. *Int J Mol Med* **41**, 3033-3040.